ENGINEERING EXPERIMENT STATION
of the Georgia Institute of Technology
Atlanta, Georgia

FINAL REPORT

PROJECT NO. 214-172

THE EFFECT OF BASE HEAT ADDITION ON THE BASE PRESSURE RATIO AND WAKE FLOW OF A TWO-DIMENSIONAL BLUNT-BASED BODY AT M = 1.98

By

RICHARD G. FLEDDERMANN

and

HURLBURT W. S. LAVIER

- o - o - o - o -

CONTRACT NO. DA-01-009-ORD-251

DEPARTMENT OF THE ARMY PROJECT: 599-01-004
ORDNANCE PROJECT: TB2-0001
OOR PROJECT: 456

Office of Ordnance Research
Birmingham Ordnance District

- o - o - o - o -

NOVEMBER, 1954

ENGINEERING EXPERIMENT STATION
of the Georgia Institute of Technology
Atlanta, Georgia

FINAL REPORT

PROJECT NO. 214-172

THE EFFECT OF BASE HEAT ADDITION ON THE BASE PRESSURE RATIO AND WAKE FLOW OF A TWO-DIMENSIONAL BLUNT-BASED BODY AT M = 1.98

By

RICHARD G. FLEDDERMANN

and

HURLBURT W. S. LAVIER

- o - o - o - o -

CONTRACT NO. DA-01-009-ORD-251

DEPARTMENT OF THE ARMY PROJECT: 599-01-004
ORDNANCE PROJECT: TB2-0001
OOR PROJECT: 456

Office of Ordnance Research
Birmingham Ordnance District

- o - o - o - o -

NOVEMBER, 1954

FOREWORD

This report was prepared by the Engineering Experiment Station of the Georgia Institute of Technology. The research reported here was sponsored by the Office of Ordnance Research under Contract DA-01-009-ORD-251.

The authors are indebted to Research Assistants Winston Boteler, Cecil Brown, Wallace Barber, Roland Culpepper, James Fry, Richard Ferster, C. M. White, and Alton Colcord; typists Marguerite Volk and Donna Williams; and machinists William C. Slocum and George Cook for their contributions to the project.

TABLE OF CONTENTS

LIST OF FIGURES

LIST OF FIGURES (Continued)

I. SUMMARY

The base pressure ratio of a blunt-based two-dimensional body at Mach No. 1.98 was very sensitive to base heat additions; the base pressure ratios increased up to 30 per cent at the highest heat inputs. This sensitivity was greatest at the low heat addition rates. The pressure ratio is asymptotic at large heat inputs due to the fluid source effect of the distributed heat input at the base.

A simplified theory of boundary layer mass transfer at the base was developed. The mass transfer coefficient k_1 developed from this theory should be larger than, but of the same order of magnitude as, that used by Lees and Crocco, reference 4. The average value for k_1 in a turbulent flow as determined from these experiments was 0.12 as compared with 0.03 by Lees and Crocco.

The stagnation temperatures in the wake near the base were 3 to 4 per cent lower than the free stream value thus indicating that the boundary layer flow, which has a low stagnation temperature value, has been carried into the wake region. For a heated wake the stagnation temperature near the base varied only slightly with distance from the base. However, four body thicknesses downstream the temperature dropped perceptibly, showing that the transfer coefficient goes up very rapidly downstream of the trailing shock. The wake stagnation pressure increased slowly with distance from the base for both the heated and unheated wake. Part of the pressure recovery is accomplished upstream of the trailing shock.

The intersection of exterior shocks with the wake produced an increase of base pressure for intersection upstream of the trailing shock. This is the same effect found by Chapman for three-dimensional bodies and shocks.

II. APPARATUS

The wind tunnel used in these experiments is an atmospheric blow-down tunnel designed to operate with a two inch by four inch test section at stagnation pressures from thirty psia to 125 psia. The test section for the experiment has a Mach number of 1.98 $\pm$ 0.02. The flow through the test section is initiated by a fast-opening valve in the line connecting the nozzle and high pressure supply tank. There are pressure taps in the test section and upstream of the throat of the nozzle.

The pressure tank has a volume of 1000 cubic feet. It is supplied by a 75 hp, 12 inch by 13 inch Worthington, type HB, horizontal, air compressor with aftercooler. The compressor furnishes 350 s.c.f.m. at 125 psi. The air from the compressor is dried by a Kemp dynamic adsorption dryer utilizing silica gel as the drying agent. It has a capacity 350 s.c.f.m. of 100°F saturated air at 125 psi for 100 minutes of operation prior to reactivation. The operating dewpoint was about -10°F.

The test model was constructed in the model shop of the Daniel Guggenheim School of Aeronautics. It is a 13° included angle wedge, 3-17/32 inches long and 2 inches wide. The top and bottom surfaces at the rear of the wedge were machined parallel to the wedge axis so that the base thickness was 0.635 inch. There are pressure taps on the top and bottom parallel surfaces and on the base. There is a cavity 1/2 inch in height and 1.0 inch deep in the base of the model to hold the heating coil. The coil is composed of 11 feet of #28 nichrome wire wound in a 3/32 inch diameter helix. This helical wire is wound about two ceramic spacers to form a long heating area. The cavity is lined with mica to prevent electrical shorting of the coil and burning of the model. At the inner wall of the cavity is a small slit which admits CO_2 to

cool the coil and prevent its oxidation. The coil heating current is supplied by a Variac. The power supply leads are brought in at either side of the cavity and connected to the coil at the rear of the model.

An exploded view of the wedge model and the coil is shown in Figure 1.

The wedge, when installed in the tunnel, spans the two inch tunnel width and is held in the test section by bosses which fit into holes drilled in the plexiglass walls of the test section. The side walls are removable to facilitate mounting of the model. The pressure leads, CO_2 supply line, and insulated heating coil leads are routed through these bosses.

The shock wave emanating from the model leading-edge upon reflection from the top and bottom walls of the test section intersected the wake two model widths downstream of the model base. This intersection caused a large error in base pressure measurements. The reflected shocks were removed by inserting two 1/16 inch tool steel plates in the test section. These plates had a 6° knife edge milled on their leading edges and were mounted parallel to the test section center line in grooves cut in the plexiglass side walls. These plates were inserted just far enough upstream to intersect the reflected shocks. A photograph of the model and shock intersector plates mounted in the test section is shown in Figure 2. One of the side walls was left off for this photograph so that the mounting details may be seen more clearly.

Temperatures were measured by thermocouples made from 0.001 inch, #40, iron-constantin thermocouple wire. Pressures were measured by Statham Laboratory pressure transducers chosen to fit the pressure range being measured. The temperature and pressure data were recorded by a nine channel, Consolidated Engineering Company recording oscillograph, type 5-116, using CEC type 7-225 galvanometers.

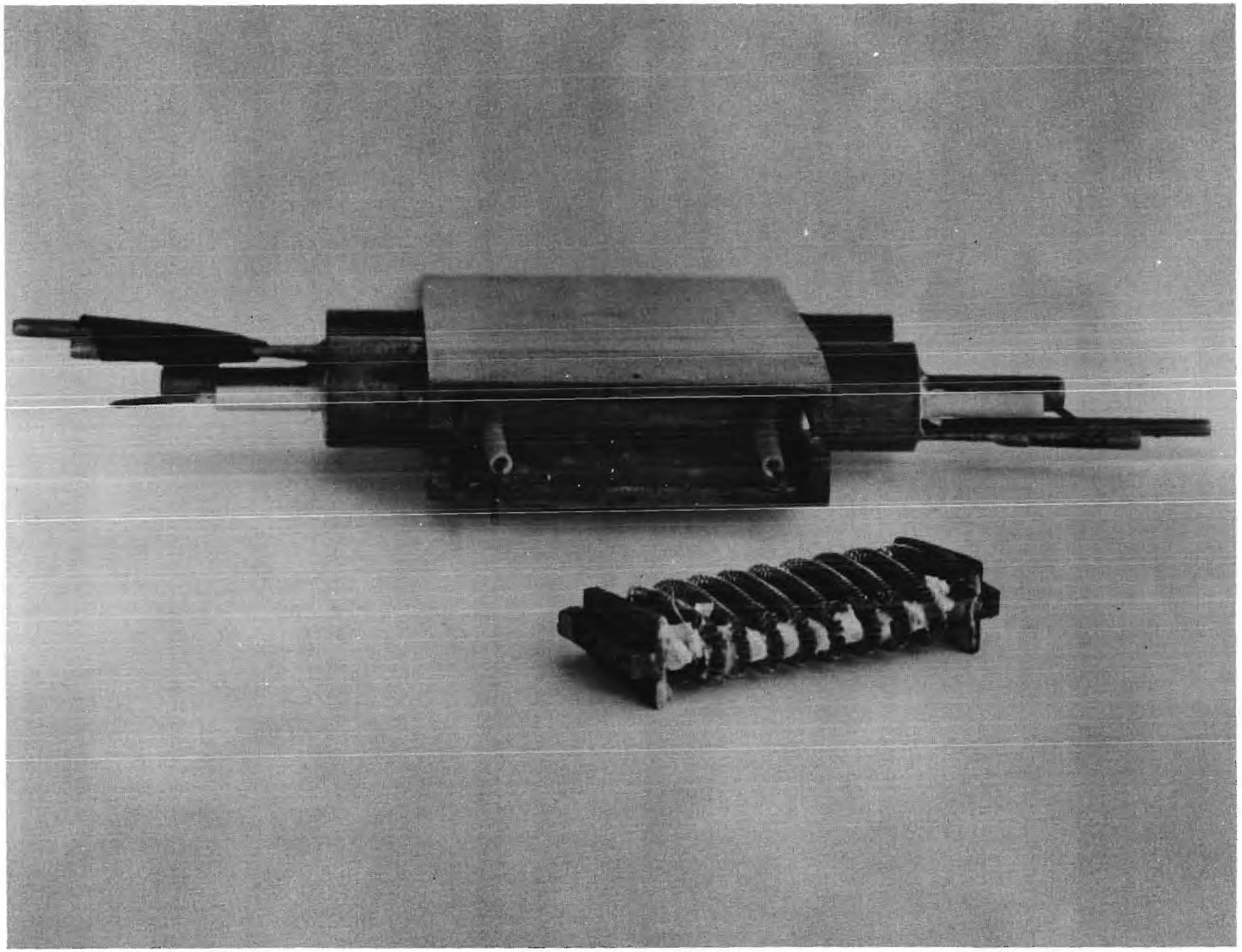

Figure 1. Exploded View of Wind Tunnel Model and Heating Coil.

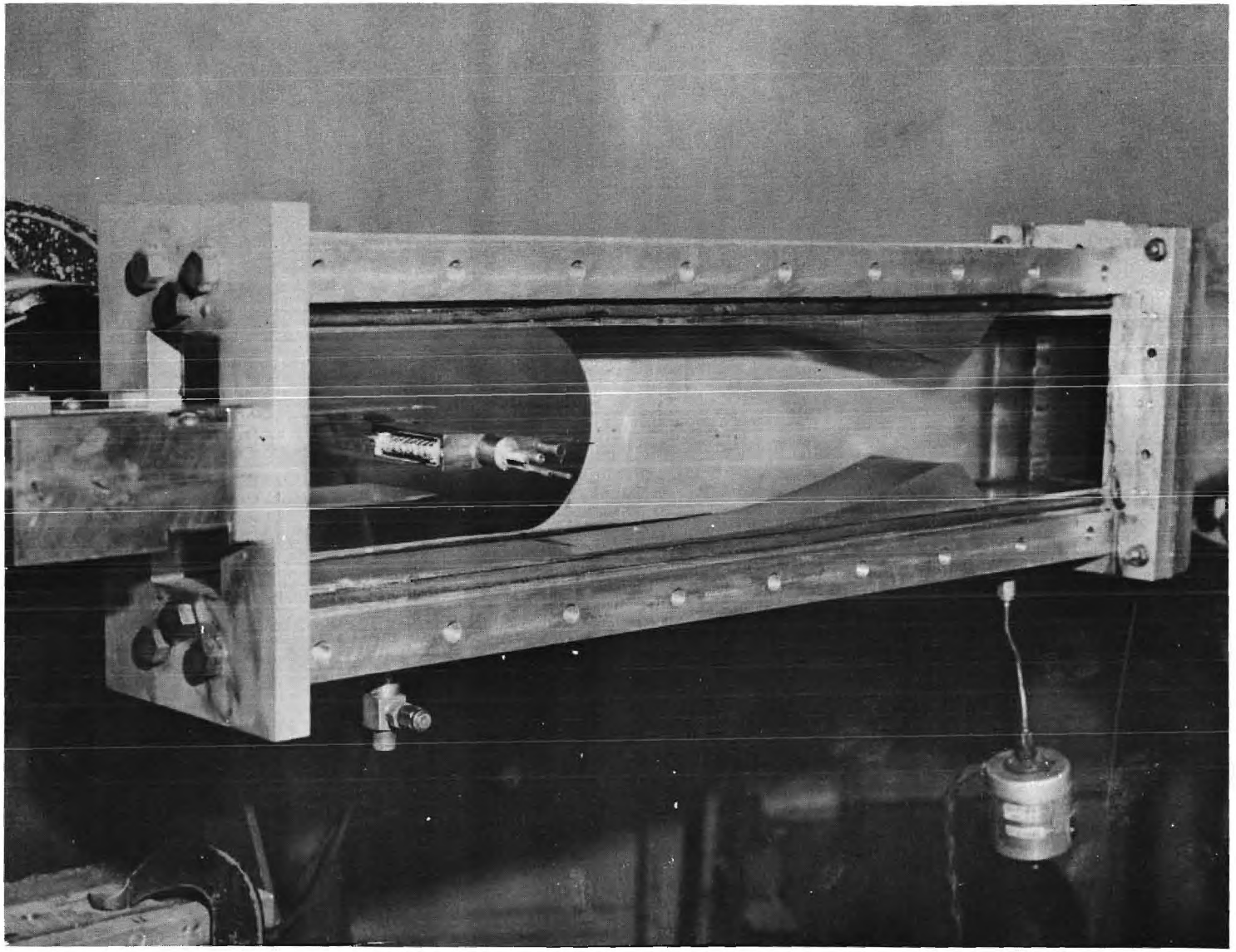

Figure 2. Model Mounted in Wind Tunnel.

The static pressure probe for measuring static pressure in the test section was 0.060 inch O.D. with a 20° conical nose; it was made from 1/16 inch stainless steel tubing. The pressure taps were located ten diameters from the nose in accordance with the data of reference 7. The stagnation pressure probe was 2-3/64 inches in length and made of 1/16 inch O.D. stainless tubing. The wake static probe was identical to the stagnation pressure probe except that the nose was filled in and rounded off; four static pressure holes, 0.012 inch in diameter, were drilled in the probe 1/4 inch from the nose.

The thermocouple probe was manufactured from 1/16 inch tubing, 1-1/16 inches in length. Four 0.010 inch breather holes were drilled in the tubing 1/8 inch from the nose. Number 40, iron-constantin thermocouple wire was pulled through the probe as far as the breather holes. The tubing was filled with insulating material as far as the breather holes to hold the wire in place.

All probes were mounted in threaded conical supports which fitted into the end of a calibrated traversing screw. The screw was supported by a wedge-shaped mount which spanned the rear of the tunnel at the centerline.

III. TEST PROCEDURE

Prior to the operation of the tunnel the pressure transducer and thermocouples to be used in the experiment were calibrated. The transducers were connected to a power source and to the recording oscillograph. A range of known pressures, produced by a vacuum pump or a pressure bottle, were applied to the transducers and the output deflection of the oscillograph recorded. From this data pressure-deflection calibration curves were drawn. The thermocouples were calibrated in a similar fashion using the temperatures of steam at standard conditions, water-ice mixture, and salt-water-ice mixture, as standard temperature points. The thermocouples were connected directly to the oscillograph. The model and the measuring probes were mounted in the tunnel. The transducers and thermocouples were mounted in place and the heating coil, if used, was connected to its power source after a continuity check.

During instrument calibration and mounting of the model the 1000 cubic feet storage tank was being pumped up to 100 psi and the air dried to a dew-point of $-10^{\circ}F$. The schlieren apparatus was turned on and adjusted for proper sensitivity.

At the time of run CO_2 was bled through the slit and the heating power was applied to the coil at the base of the model (this was omitted for cold runs). The on-off gate valve was opened and the tunnel was operated until the base free surface flow, as observed on the schlieren screen, opened outward from its normal turned in position. Schlieren photographs were taken as desired during the run. The pressure tank was pumped up at this time to prepare for the next run.

After the run the oscillograph record and schlieren negatives were developed in the darkroom. The pressure-temperature data were reduced from the oscillograph record utilizing the calibrations taken prior to the run.

IV. THEORY

The Prandtl boundary layer theory is based upon the physical fact that for fluid flow over a surface there is near the surface a definite, thin layer. This layer is characterized by rapid change of fluid velocity from zero at the surface to its free stream value at the edge of the layer. The governing hypothesis of the theory is that the ratio of the boundary layer thickness to length of the surface is small compared to unity. Symbolically, this is $\delta/\ell \ll 1$, where δ is the layer thickness and ℓ is the length of surface. This hypothesis led to a simplification of the Navier-Stokes equations of motion by neglecting all terms of order δ or smaller. Solutions of the simplified or boundary layer equations of motion abound in fluid mechanics literature. The majority of these solutions leave much to be desired in the vicinity of the separation point. The position of the separation point can only be fixed approximately. Moreover, no complete solution is known for the flow within the separated region. The mathematical difficulty rests in great part upon the fact that the separating of the flow from the surface produces a mathematical singular point at separation and the physical thickening of the flow in this region leads to values of δ/ℓ which violate the $\delta/\ell \ll 1$ hypothesis of the boundary layer equations of motion.

Goldstein, reference 5, made a notable advance toward the solution of the flow near the separation point. He noted that the classic Blasius solution for flow over a flat plate had a singular point at the leading edge of the plate. Carrier and Lin, reference 1, had removed the singular point by a change of coordinates from Cartesian to parabolic. They found that the Blasius solution was correct everywhere except in a limited region near the leading edge. Thus the Blasius solution, an expansion about the singular point, was

correct away from the singular point; moreover, the singular point was a fictitious one which depended upon the coordinate choice. Goldstein started with the assumption that a series solution could be obtained about the separation point, $x = x_s$.

The formal solution was accomplished by non-dimensionalizing the equation of motion to

$$u_1 \frac{\partial u_1}{\partial x_1} + v_1 \frac{\partial u_1}{\partial y_1} = U_1 \frac{dU_1}{dx_1} + \frac{\partial^2 u_1}{\partial y_1^2}$$

where $x_1 = (x - x_s)/L$, $y_1 = R^{1/2} y/L$, $u_1 = u/U_s$,

$v_1 = R^{1/2} v/U_s$, $U_1 = U/U_s$, $\psi_1 = R^{1/2} \psi/LU_s$

and the subscript s refers to the separation point. R is the Reynolds number defined as $U_s L/\nu$ and L is a representative length given by $L = -U_s/U_s'$. The stream function is defined to give

$$u_1 = \frac{\partial \psi_1}{\partial y_1}, \qquad v_1 = -\frac{\partial \psi_1}{\partial x_1}$$

The boundary conditions downstream of separation were taken as $u_1 = v_1 = 0$ at $y_1 = 0$ (wall) and $u_1 = U_1$ at $y_1 = \delta_1$.

One major conclusion of Goldstein was that at $x_1 = 0$ the velocity distribution is given by

$$u_1 = \frac{1}{2} y_1^2 - \frac{1}{6} \alpha_1^2 y_1^4 + \frac{2^{1/2} \pi \alpha_1^3}{40 (\frac{1}{4}!)^2} y_1^5 + \cdots \qquad (1)$$

where α_1 is a constant sensitive to the flow upstream of separation. Equation 1 may be thought of as a new boundary condition for $x_1 = 0$.

Equation 1 was derived utilizing an asymptotic series expansion for ψ_1, and considering the convergence of the various terms of the series at infinity. The expression for ψ_1 is

$$\psi_1 = 2^{3/2} \xi^3 \left[F_0(\eta) + \xi F_1(\eta) + \xi^2 F_2(\eta) + \cdots \right] \qquad (2)$$

where $\xi = x_1^{1/4}$, $\eta = y_1/2^{1/2} x_1^{1/4}$

Further

$$U_1 \frac{dU_1}{dx_1} = 1 + P_1 x_1 + \tfrac{1}{2} P_2 x_1^2 + \cdots \qquad (3)$$

Goldstein concluded that the flow downstream of the separation point was complex for a real flow upstream. Hence no downstream solution is possible. This points up the fact that the large boundary layer thickness downstream of separation destroys the assumption, $\delta/\ell \ll 1$, which underlies the equation of motion.

Stewartson, reference 8, utilized the same asymptotic expansion and pressure gradient as Goldstein, equations 2 and 3. Physically, there is a free surface starting from the stagnation point and extending into the stream. There is an extensive, so-called, dead air region extending from the body surface to the fluid free surface. Stewartson moved the lower boundary condition from the body surface to the free surface. Thus the thickness δ is considerably decreased. Stewartson was able to solve the asymptotic equations downstream using equation 1 as an initial boundary condition. In this way he arrived at the equation of the free surface and the velocity distribution along it. However, there was nothing definite about it as the solutions were in terms of a group of complicated functions and constants of integration, which arose out of the asymptotic series. The exact determination of these constants appears to be very difficult.

Stewartson's solution was made for a pressure gradient of the form of equation 3. The dead air region is usually a region of constant pressure although a pressure gradient could be supported by a vortex situated in the region. He was unsuccessful in applying Goldstein's method to the zero

pressure gradient case, which is unfortunate as this would be close to reality. The authors attempted a solution of this case by modifying the asymptotic series and by utilizing an expression for the pressure gradient which would approach zero in the limit (e.g. $p_0 e^{-Sx_1}$ for large values of S). All the methods tried by the authors failed at some approximation of equation 1 at $x_1 = 0$. The stumbling block appeared to be the zero coefficient of the y_1^3 term in equation 1.

It is unfortunate that the solution of the zero pressure gradient case is so elusive. The solution of the incompressible case could be transformed into the compressible case through use of the Stewartson transformation, reference 9. The experiments, of which this report deals, are concerned with the flow at the base of a two-dimensional, blunt-based body in a supersonic flow. The free surface adjacent to the base is essentially a straight line and has a nearly zero pressure gradient along it. The solution of the zero gradient case would be invaluable in determining the mass transfer properties along the free surface. This mass transfer is the crux of the base pressure problem.

Lees and Crocco, reference 4, approached the problem in a different way. They started with the von Karman integral relation rather than the boundary layer equations of motion. They found that two parameters κ and f, where $f = f(\kappa)$, controlled the boundary layer solutions. The definitions of f and κ are given by

$$\kappa \equiv \frac{\delta_i - \delta_i^* - \delta_i^{**}}{\delta_i - \delta_i^*} \tag{4}$$

and

$$f \equiv \frac{(\delta_i - \delta_i^* - \delta_i^{**})\delta_i}{(\delta_i - \delta_i^*)^2} \tag{5}$$

for which δ_i = the incompressible boundary layer thickness,

δ_i^* = the incompressible displacement thickness,

δ_i^{**} = the incompressible momentum thickness.

They plotted the $f - K$ curves for known boundary layer solutions and found that there was a general trend toward one curve as the flow approached the separation point. Moreover, in a free jet $f = K = 1$. The separated flow lies, as was tacitly assumed by Stewartson, between the free jet and attached boundary layer cases. Lees and Crocco assumed a plausible $f - K$ curve which fits between the curve for an attached boundary layer and $f = K = 1$. With this technique it would not be possible to predict the flow with any quantitative accuracy. However, qualitatively they found good agreement. Quantitative agreement must await experimental determination of the proper $f - K$ curve.

The physical picture of the flow of a compressible gas at $M > 1$ over the rear of a blunt-based two-dimensional body is shown in Figure 3.

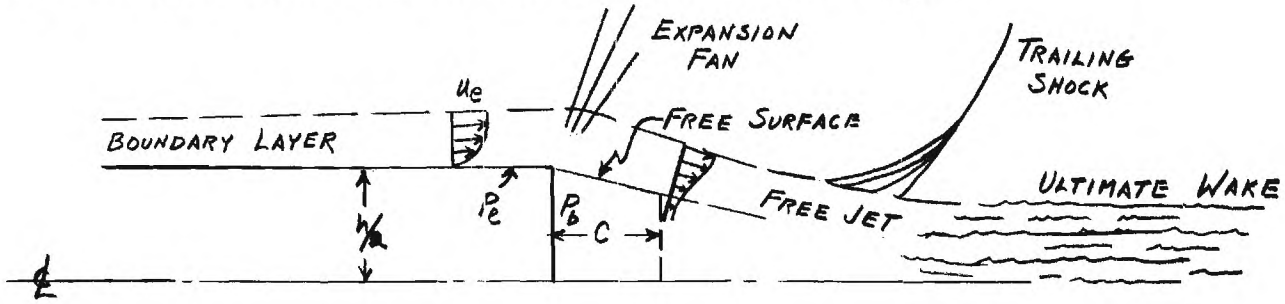

Figure 3. Flow Over Upper Half of Blunt-Based Body at Supersonic Speed.

The boundary layer is turned at the base by a Prandtl-Meyer expansion. Initially the free surface is a straight line. However, the slow recovery of pressure in the wake induces curvature in the free surface. The compression

Mach lines emanating from this curved surface coalesce to form the trailing shock and turn the flow back parallel to the free stream.

The base pressure is dependent upon the initial angle of turn of the separated flow. There is an infinity of angles of turn smaller than some maximum limiting angle (the limiting angle is dependent upon the ability of the trailing shock to turn the flow parallel to the free stream once again). There must be a physical reason why the flow picks out one particular value of base pressure. This can be traced to the transfer of mass across the free surface from the boundary layer to the base region. There must be a mechanism which controls this mass transfer. One of the important contributions of Lees and Crocco was a mathematical demonstration of the control mechanism.

They assumed that the mass transfer rate could be given by

$$\frac{d\bar{m}}{dx} = k_1 \rho_e u_e \qquad (6)$$

where $\bar{m}$ = the mass per second flowing in the boundary layer,

k_1 = the mass transfer coefficient,

e = a subscript referring to the stream external to the boundary layer. Insertion of equation 6 into the compressible von Karman integral relation reduced the relation after some juggling to a linear differential equation (e.g. 2.30 of ref. 4). This equation exhibited a singular point under all conditions. Careful calculations showed that this singular point was physically within the wake in the vicinity of the trailing shock. It acts mathematically in the same fashion as the throat of a supersonic nozzle to control the flow. There is experimental evidence, which will be discussed in another section, to indicate that this mathematical singular point exists as a real critical point.

The flow near the surface of the body is a typical boundary layer flow.

This type of flow continues up to the separation point at the base. Far downstream of separation the dissipative boundary layer flow has taken on the characteristics of a free jet. There is some region in between where the dissipative flow is changing character from pure boundary layer flow to free-jet flow. Another significant result of the Lees and Crocco theory is that the flow changes character within a length two boundary layer thicknesses from the base. Symbolically this length is 2δ.

The theory shows that the base pressure is a function of both $\bar{m}$ and k_1. As k_1 depends upon whether the flow is laminar or turbulent and $\bar{m}$ is a function of δ, the results should be sensitive to Reynolds number and the state of turbulence of the flow. Lees and Crocco found that the theory did predict the shape of the base pressure-Reynolds number curve although the exact values were in considerable error. A by-product of the theory shows that the ratios of base pressure to free stream pressure is a function of δ/h where h is the thickness of the base. This had previously been predicted experimentally by Chapman, reference 2.

The paper of Lees and Crocco is a splendid advance toward an understanding of base pressure phenomena. It uses a logical physical approach and predicts qualitatively many of the known phenomena. The mathematics shows that there is a critical, throttling section in the wake, which occurs in the vicinity of the trailing shock. This was unsuspected from the previous experimental data. Confirmation of this theory awaits a better understanding of the mixing coefficients and the flow at the base. The authors of this report have attempted to determine this mixing coefficient (at least for turbulent or near turbulent flow) by means of a simplified approach which will be explained in the paragraphs to follow.

The mass transfer coefficient, k_1, of equation 6 may lead to a little confusion. This can be traced to the term $d\bar{m}/dx$. This term represents the rate of change of mass within the boundary layer per unit distance for a two-dimensional flow. This does not represent the transfer of mass to the dead air region but is the difference between the mass added to the free boundary layer and that subtracted by addition to the dead air region. The mass transfer coefficient would actually be higher than k_1. This confusion may be obviated by defining a new coefficient k in the following manner.

$$\frac{dm}{dt} = \rho_e u_e \delta^* k \tag{7}$$

where dm/dt is the mass transferred per second to that part of the dead air region, which most directly affects the base pressure, and δ^* is the displacement thickness of the boundary layer at separation (base). It is assumed that the mass transferred per second, dm/dt, in the two-dimensional flow is fed into a small volume, ch/2, adjacent to the base; see Figure 3. The length c is not specified except that it is small. It may be loosely defined as a minimum length beyond which the mass transfer does not appreciably affect the base pressure.

Thus $k_1 \leq k\delta^*/c$, the exact value depending upon the rate of addition of mass from the exterior flow into the free boundary layer. If we assume c is equal to the critical length, 2δ , in which the dissipative flow is changing character from boundary layer flow to free jet flow, then

$$k_1 \leq 0.5\, k\delta^*/\delta$$

Assume that initially the volume ch/2 is empty and is being filled (or actually maintained) at a rate dm/dt given by equation 7. The density, ρ_b , at the base is reached in a time t_o which we shall call the filling time.

This is given by

$$\rho_b = \frac{2}{ch} t_o \frac{dm}{dt} \tag{8}$$

The subscript b will be used to denote quantities in the dissipative flow near the base. Utilizing the equation of state and solving for t_o, one obtains

$$t_o = \frac{ch}{2} \frac{p_b}{RT_b} \frac{1}{dm/dt} \tag{9}$$

This can be reduced by use of equation 7 to

$$t_o = \frac{ch}{2} \frac{p_b}{RT_b} \frac{1}{\rho_e u_e \delta^* k}$$

This may be reduced further by application of the equation of state to the external stream. The filling time is then

$$t_o = \frac{ch}{2k u_e \delta^*} \frac{T_e}{T_b} \frac{p_b}{p_e} \tag{10}$$

A non-dimensional time $\bar{t}$ may be defined from equation 10 by

$$\bar{t} = \frac{1}{2k} \frac{h}{\delta^*} \frac{T_e}{T_b} \frac{p_b}{p_e} \tag{11}$$

where $\bar{t} = u_e t_o / c$

In passing it can be seen that $\bar{t}$ may be considered as either a non-dimensional time or a non-dimensional velocity.

Solving equation 11 for the ratio of base pressure to free stream pressure one arrives at the important result.

$$\frac{p_b}{p_e} = 2k\bar{t} \frac{T_b}{T_e} \frac{\delta^*}{h} \tag{12}$$

This is an analytical expression of Chapman's experimental result, references 2 and 3, that P_b/P_e may be correlated with δ^*/h. The variation from linearity at any particular external Mach number would be caused by a variation of k or $\bar{t}$ as $T_b/T_e \approx 1 + \frac{\gamma-1}{2} M_e^2$.

The change in base pressure ratio with heat addition at the base may be handled by a similar analysis to that which led to equation 12. We make the assumption that heat is added at constant volume to the volume ch/2 for a time t_o. Under this condition the base pressure will rise from a pressure P_b with no change in density. Thus

$$p_b' = \rho_b R T_b' = \rho_b R (T_b + \Delta T)$$

or

$$\frac{p_b'}{p_e} = \frac{p_b}{p_e} + \frac{\rho_b R \Delta T}{p_e} \tag{13}$$

The base pressure ratio after addition of heat is simply the no-heat ratio plus an increment due to heat. As heat is added at constant volume

$$dQ = C_{v_s}\, dT$$

where Q is heat added and C_{v_s} is the heat capacity at constant volume of the mass in the volume ch/2. Therefore

$$\frac{dQ}{dt} t_o = C_{v_s} \frac{dT}{dt} t_o = C_{v_s} \Delta T$$

or

$$\Delta T = \frac{t_o}{C_{v_s}} \frac{dQ}{dt} \tag{14}$$

The heat capacity per unit mass C_v is given by $C_v = C_{vs}/m_s$ where m_s is the mass in ch/2. Utilizing this fact

$$C_v = \frac{2 C_{v_s}}{\rho_b c h} \qquad \text{or} \qquad C_{v_s} = \frac{\rho_b c h C_v}{2}$$

Equation 14 reduces to

$$\Delta T = \frac{2 t_o}{\rho_b c h C_v} \frac{dQ}{dt}$$

and the pressure ratio increment becomes

$$\frac{\rho_b R \Delta T}{p_e} = \frac{\rho_b R}{p_e} \frac{2t_o}{\rho_b c h C_v} \frac{k}{k} \frac{dQ}{dt}$$

$$= 2k\bar{t} \frac{R}{p_e u_e h C_v k} \frac{dQ}{dt}$$

Introducing a new quantity $Q_n = Q/h$, where Q_n is the heat added per unit area of base, the equation for p_b'/p_e may then be written as

$$\frac{p_b'}{p_e} = 2k\bar{t} \left[\frac{T_b}{T_e} \frac{\delta^*}{h} + \frac{R}{p_b u_e C_v k} \frac{dQ_n}{dt} \right] \tag{15}$$

k and $\bar{t}$ may be found from equation 15 utilizing the data for base pressure ratio with and without heat.

V. EXPERIMENTAL RESULTS

The main purpose of the experiments, reported herein, was to determine the effect of base heat addition upon the base pressure ratio. The principal experimental difficulty arose from having to add heat at the base without introducing large effects due to fluid momentum. This precluded the simple arrangement of blowing hot air out of an opening in the base of the model. The final system, as described in detail in section II, consists of a heating coil capable of handling 1200 watts inserted in the rear of the model. This coil was protected from oxidation by a small amount of CO_2 flowing around it. The momentum effect of the CO_2 was negligible. This can be seen in Figures 4 and 5 which are plots of base pressure ratio and stagnation pressure ratio in the wake, for CO_2 added and not added with no heat addition. The scatter of the data is commensurate with the usual accuracy of separate runs. All data were taken at a Mach number of 1.98.

The insertion of the coil in the base of the model necessitated a model with a thick base. The thickness of the first model was chosen as a compromise between base thickness and blockage of the 2" x 4", M = 1.98, blowdown tunnel. Due to boundary layer build-up on the walls of the tunnel and on the model, the tunnel blocked. The blocking caused separation of the tunnel wall boundary layer at the nozzle inflection point and produced transonic flow over the surface of the model. The model was shaved down until the flow was no longer blocked. The shaving process rendered the model unfit for taking pressure data due to uncovering of pressure lines. A new model was built, whose thickness was slightly smaller than the critical size determined from the first model. The thickness could not be made much less than critical thickness due to the size of coil required. Reasonable care had to be taken, when using

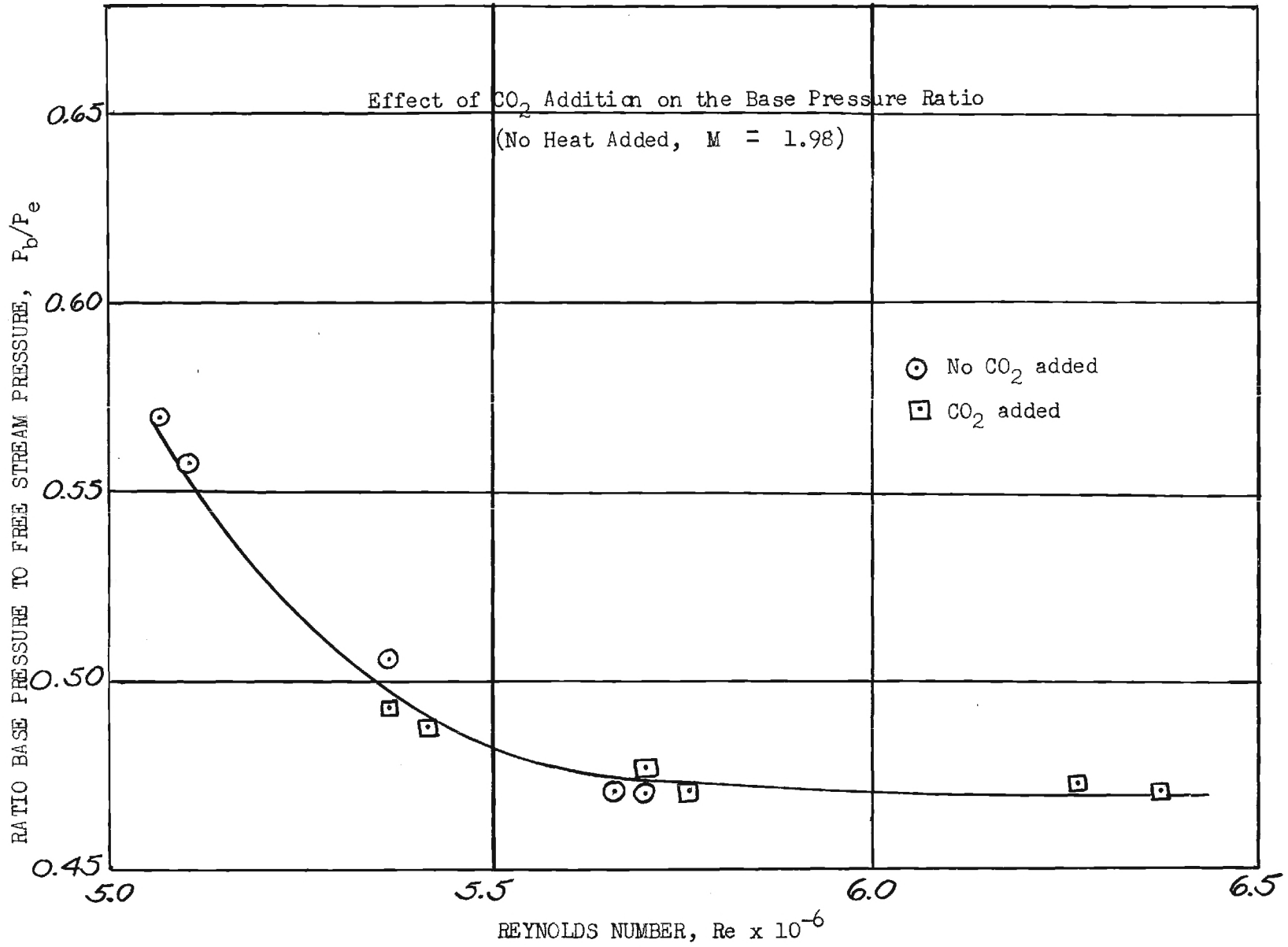
Effect of CO_2 Addition on the Base Pressure Ratio
(No Heat Added, M = 1.98)
No CO_2 added
CO_2 added
RATIO BASE PRESSURE TO FREE STREAM PRESSURE, P_b/P_e
0.65
0.60
0.55
0.50
0.45
5.0
5.5
6.0
6.5
REYNOLDS NUMBER, Re x 10^{-6}

Figure 4

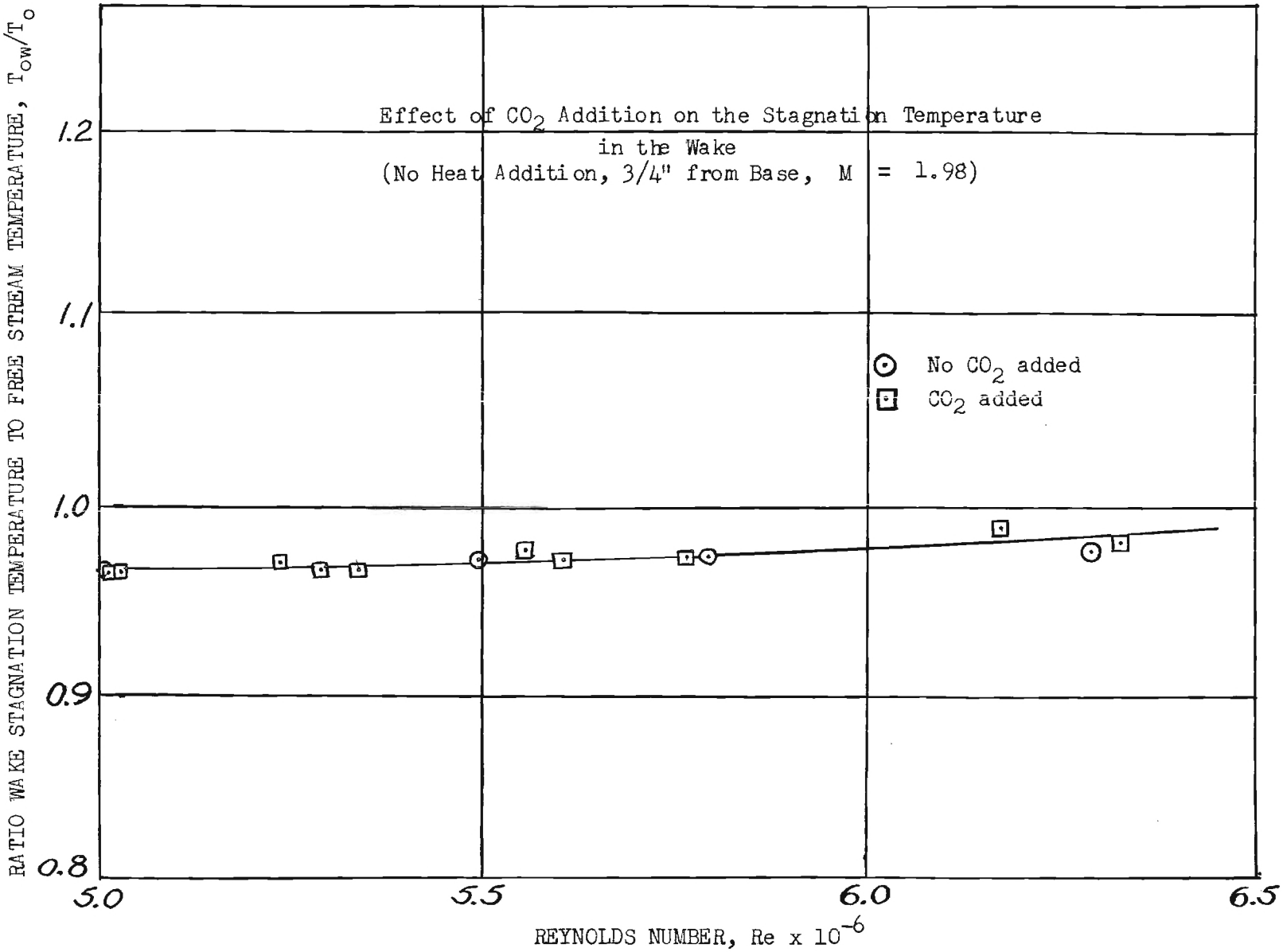
Effect of CO_2 Addition on the Stagnation Temperature
in the Wake
(No Heat Addition, 3/4" from Base, M = 1.98)
No CO_2 added
CO_2 added
RATIO WAKE STAGNATION TEMPERATURE TO FREE STREAM TEMPERATURE, T_{ow}/T_o
1.2
1.1
1.0
0.9
0.8
5.0
5.5
6.0
6.5
REYNOLDS NUMBER, Re x 10^{-6}

Figure 5

the coil, to prevent it shorting out. The coil cavity was lined with mica and mica was inserted between some parts of the coil. This added to the size of the heater and thus to the base thickness of the model.

The second model did not block the tunnel. However, another phenomenon occurred; the nose shock after reflection from the wall of the tunnel intersected the wake about two model thicknesses downstream of the base. This increased the base pressure to a value such that a shock wave, instead of the usual Prandtl-Meyer expansion, attached itself to the trailing edge. The shock wave induced separation of the model boundary layer at the trailing edge and produced thickening of the boundary layer at this point. A schlieren photograph of this flow at $M = 1.98$ is shown in Figure 6. Due to the diffuseness of the reflected shock and the thickening of the free boundary layer the reproduction does not show as much detail as would be desirable.

Figure 7 is a schlieren photograph of the base region for no flow. This figure is included with Figure 6 for purposes of comparison. The parallel thick black lines are the grooves in the wall used for mounting the shock interception plates.

Chapman, reference 2, performed an experiment to determine the effect of a reflected shock upon the base pressure ratio of a three-dimensional, cone-cylinder combination model placed in a supersonic stream. The reflected shock was simulated by the nose shocks of two small cones placed above and below the base of the model. The axial position of the small cones could be varied so that the nose shocks could be made to intersect any selected portion of the wake. Chapman only reported two tests for the shocks intersecting 2.5 and 0.9 model diameters to the rear of the model. In the first case there was no change in base pressure. However, for the 0.9 diameter case there was an

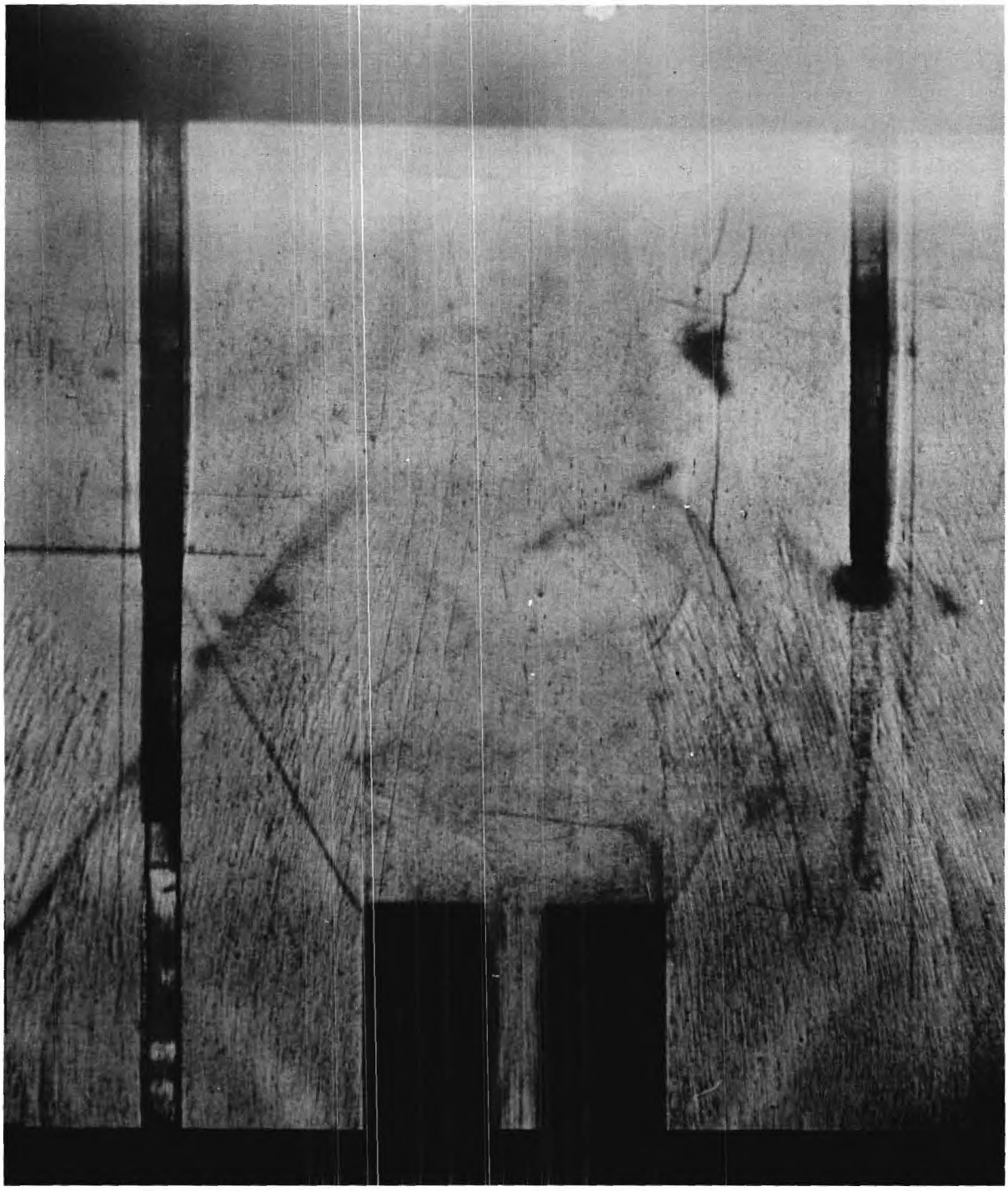

Figure 6. Schlieren Photograph of Flow at Base, Flow Turning Out, M=1.98.

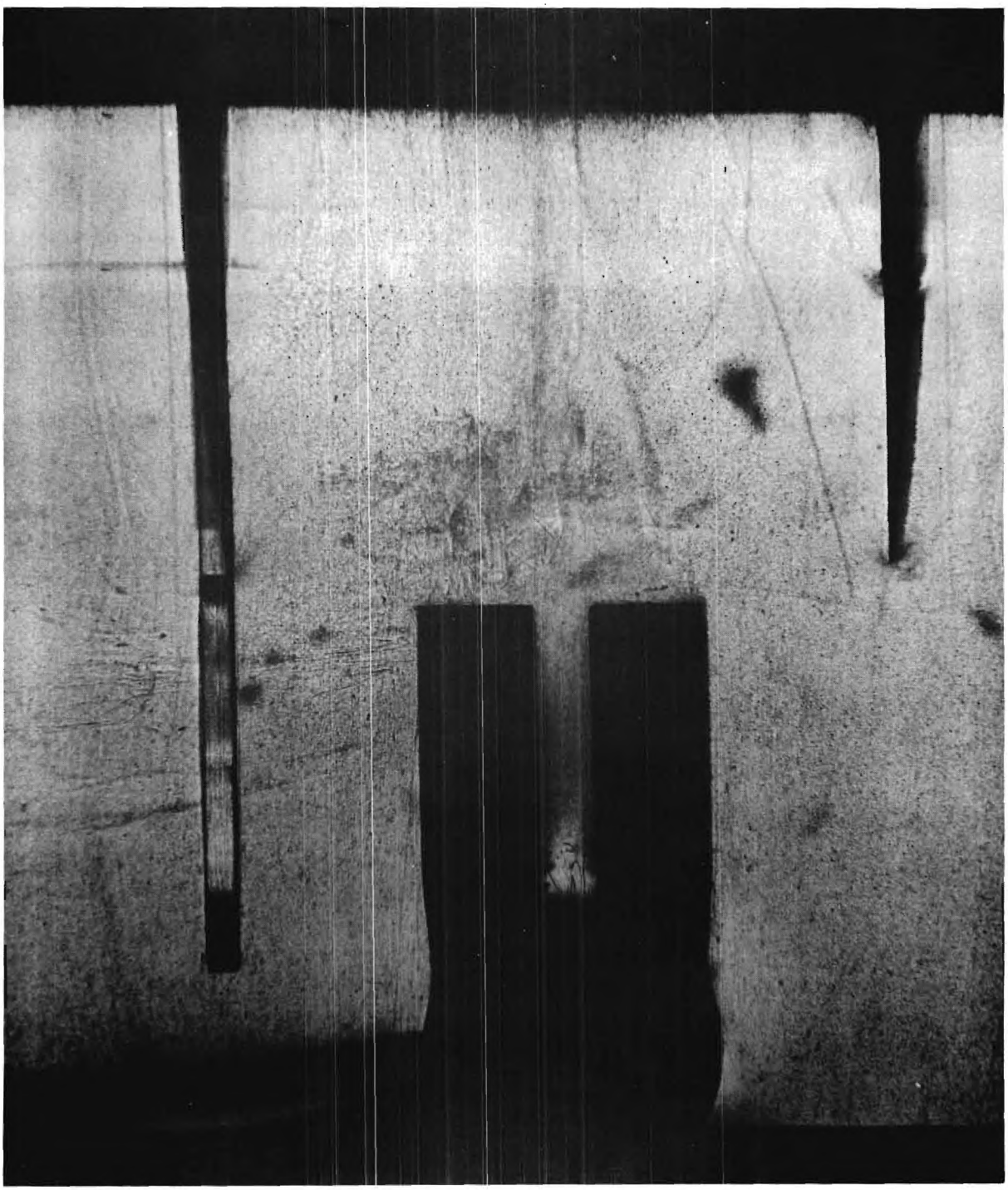

Figure 7. Schlieren Photograph of Base Region, No Flow.

appreciable increase in base pressure. In the two-dimensional case, discussed in the previous paragraph, the base pressure was increased by a reflected shock intersecting the wake about two base thicknesses downstream of the base. This is similar to Chapman's results, when one considers that the two-dimensional shock is stronger than the three-dimensional one.

In order to get the true base pressure the reflected shock had to be removed. A 6° cut was made on one surface of a piece of 1/16 inch tool steel to form a flat plate with a thin wedge at its extremity. Two of these plates were mounted parallel to the tunnel center-line in grooves cut 1.5 inches apart in the plexiglass tunnel walls. The plates were mounted so that the flat sides were toward the wake and the wedge portions intercepted the reflected shock. This set up is shown in Figure 2. It was hoped that the leading edge shock from the wake side of the plates would be so weak that it would not affect the flow appreciably. Figure 8 is a schlieren photograph of the wake flow with the plates inserted. The wake flow is now turned inward at the base thus producing the expected low base pressure.

This increase in base pressure is unexpected. When a shock intersects the surface of a free jet, it reflects as a Prandtl-Meyer expansion due to the boundary condition of uniform pressure across the free surface. For this case where equal strength shocks intersect at the same distance from the base on either side of the wake, the free surfaces would converge the wake free surfaces inward. As the wake is subsonic this would tend to decrease the pressure rather than raise it. Yet the pressure increase is of the order of 80 per cent for some cases tested. This anomaly may be explained by the existence of the Lees and Crocco critical section. If the shock intersects downstream of this section, the upstream flow is unaffected, as Chapman found.

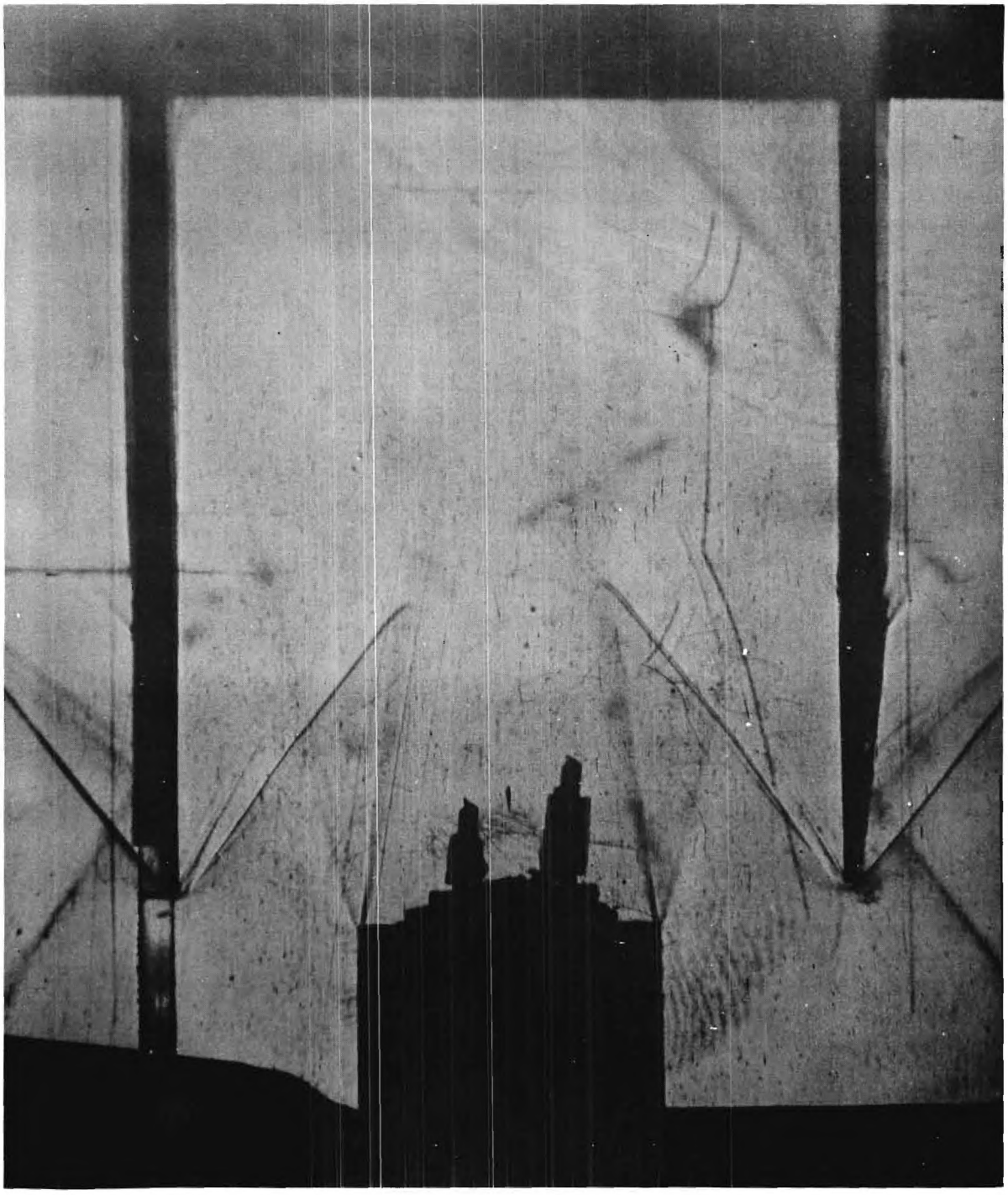

Figure 8. Schlieren Photograph of Flow at Base, Flow Turning In, No Heat Added, M=1.98.

However, for upstream intersection the mass transfer conditions at the critical section would be changed due to the changed free surface conditions downstream of the shock. However, the negatives of Figures 6 and 8 show that the free surface angle after shock intersection in Figure 6 is of the same order of magnitude as the angle for the flow of Figure 8, where the flow turned inward at the base. It appears likely that the critical section tends to maintain a similar flow in its vicinity regardless of the position of the upstream shock. If we assume the same free surface angle at the critical section, the free surface turn angle at the base must be less for the shock intersection case due to the extra angle of turn at intersection. This smaller angle of turn increases the base pressure. Unfortunately, the small size, 2" x 4", of the wind tunnel used for these tests and its sensitivity to blocking did not permit any further investigation of the critical region and its dependence upon external disturbances.

The above discussion of base pressure increase with shock intersection may be described in a different way. The critical section tends to pass the same mass flow whether the shock has intersected the wake or not. When the shock tends to turn in the wake, it narrows the critical section. A higher base pressure is needed to push the same mass flow through the critical section.

As the tunnel used for these experiments was a blow-down type with no pressure control, the stagnation pressure and Reynolds number of the flow dropped continuously during a run. Consequently, the mass transfer effects and the boundary layer thickness were not constant throughout a run. At the beginning of a typical run the free surface was turned inward and there was a minor oscillation of a small measuring probe placed in the dead air region. At some point during the run the steadiness disappears and the probe oscillates

violently. The oscillograph record of wake pressure and temperature versus time during the run showed a definite kink for this point. Then the oscillation died away and shortly thereafter the free surface opened outward. This oscillation period appears to be a transition period from turbulent to laminar flow; the weak shock emanating from the shock interception plates is now strong enough to affect the wake and cause the free surface to open outward. The data presented in this paper were limited almost exclusively to the turbulent flow region for which the free surface turned inward.

The ratio of base pressure to free stream pressure as a function of the Chapman parameter, $\ell/h\ (Re_\ell)^{1/5}$, is plotted in Figure 9 for amounts of heat added at the base from 0 to 1187 watts. The Reynolds number range is 5.7×10^6 to 6.8×10^6. It can be seen from the data that there is a decided increase in base pressure with heat addition, up to about 30 per cent for the 1187 watts case. Figure 10 is a schlieren photograph of the wake flow with 1187 watts heat addition; it shows no significant change from the no heat photograph. The small probe oscillation, which characterizes the no heat flow, disappears for heat inputs of 420 watts and above; the addition of large amounts of heat apparently stabilizes the wake flow. It can be seen that the increase of base pressure ratio is most sensitive to small amounts of heat.

This base pressure rise with heat addition is mainly a function of two opposing effects. The first is the rise in pressure akin to adding heat to a closed system. The second is the increase in wake velocity with consequent pressure drop caused by the direct analogy of a heat source with a fluid source. Hicks, Hebrank and Kravitz, reference 6, have shown that a heat source acts in the same way as a fluid source in changing the velocity of a moving air

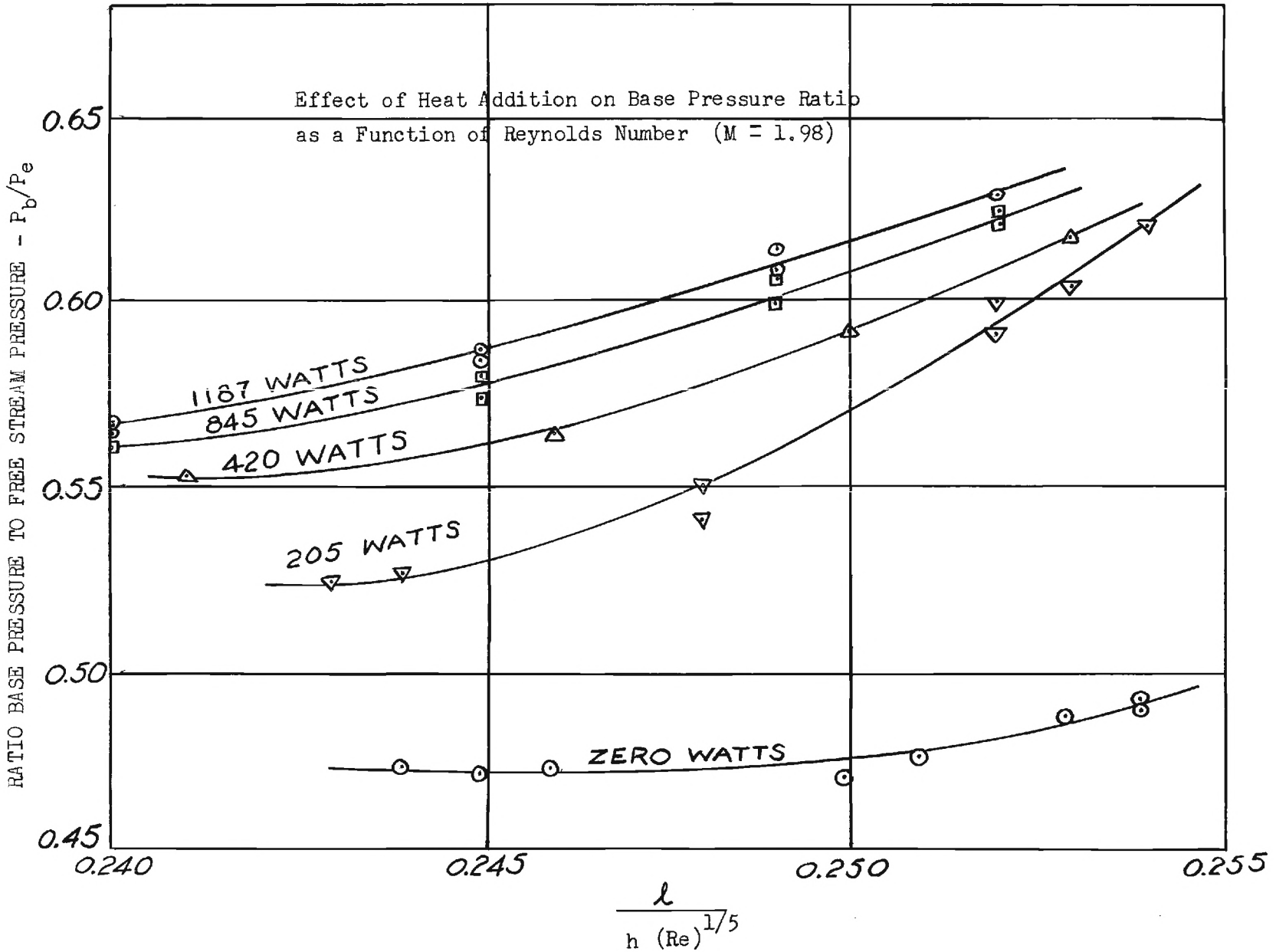
Effect of Heat Addition on Base Pressure Ratio
as a Function of Reynolds Number (M = 1.98)
RATIO BASE PRESSURE TO FREE STREAM PRESSURE - P_b/P_e
0.65
0.60
0.55
0.50
0.45
1187 WATTS
845 WATTS
420 WATTS
205 WATTS
ZERO WATTS
0.240
0.245
0.250
0.255
$\frac{l}{h\ (Re)^{1/5}}$

Figure 9

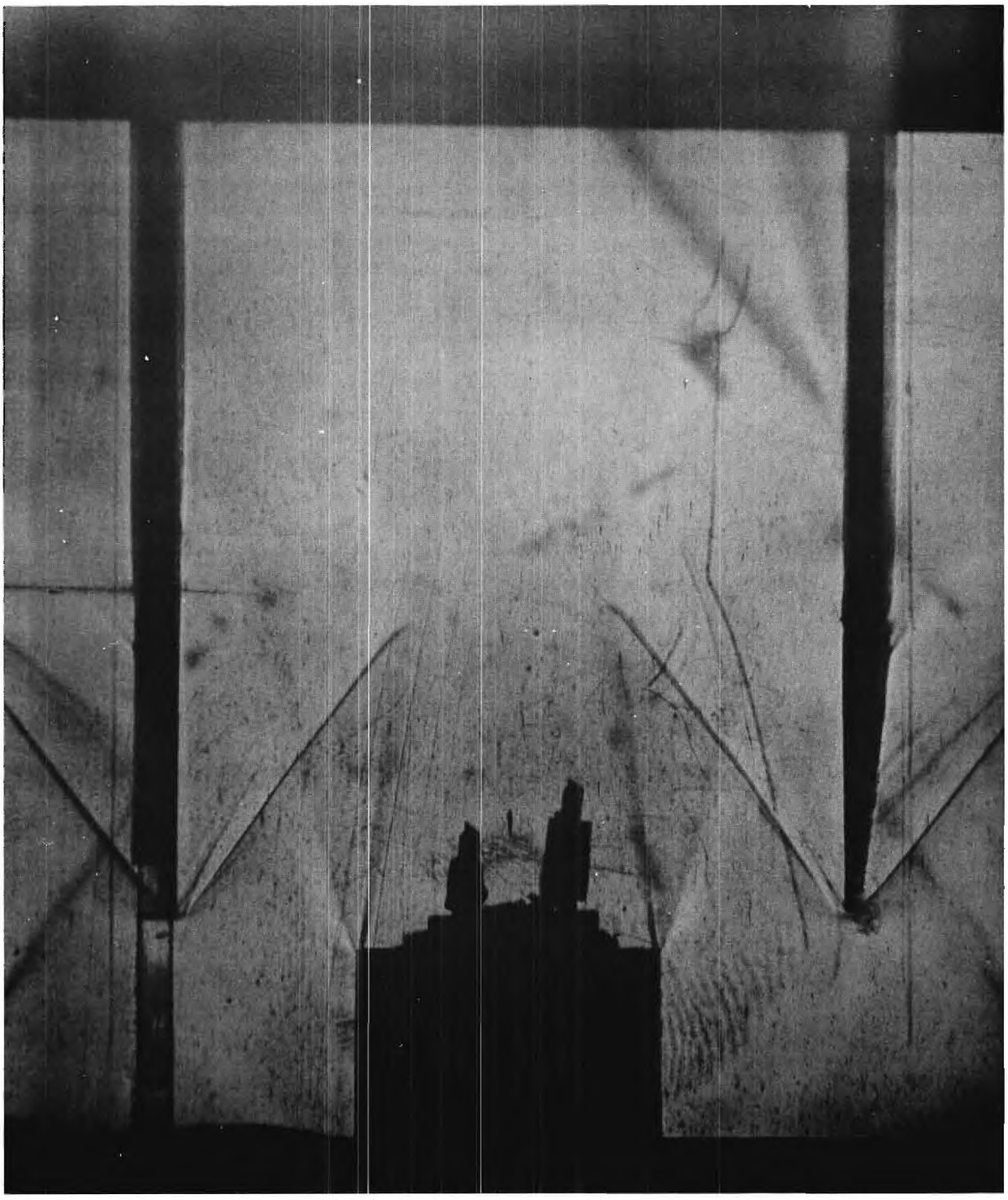

Figure 10. Schlieren Photograph Flow at Base, Flow Turning In, 1187 Watts Heat Addition, M=1.98.

stream. The closed system pressure rise is linear. The base pressure is maintained by a mass transfer across the free surface; this transfer is characterized by an average transfer velocity. The heat source produces a velocity which bucks the transfer velocity. The resultant transfer velocity is lower and is the vector sum of the zero heat transfer velocity and the heat source velocity. This produces a non-linear reduction in base pressure whose effect increases with heat addition.

In order to find k and $\bar{t}$ equation 15 is used. If the values of k and $\bar{t}$ are to be quantitatively correct the slope of the base pressure ratio versus heat addition curve at zero heat addition is utilized to reduce the effect of heat induced velocities on the free surface mixing. Figure 11 is a cross plot of Figure 9 with Reynolds number as parameter. It indicates more fully the non-linearity of the heat addition and is used to find the slopes at zero heat addition.

The values of k and $\bar{t}$ as determined from equation 15 are plotted in Figure 12. The values of δ^* used in equation 15 were computed for the 1/7 power subsonic velocity distribution corrected for Mach number by

$$\delta^* = \delta^*_{subsonic}\left[1 + \frac{1.03}{5.2}(\gamma-1)M^2\right] \qquad (16)$$

The correction amounted to 30 per cent for M = 1.98. The values of k and $\bar{t}$ are slowly varying over the limited Reynolds number range of the tests. Due to the difficulty of determining accurate slopes from the base pressure ratio-heat addition curves, one could assume that they were essentially constant in this region.

The distance, C, had been defined earlier as the minimum length beyond which the mass transfer does not appreciably affect the base pressure. If

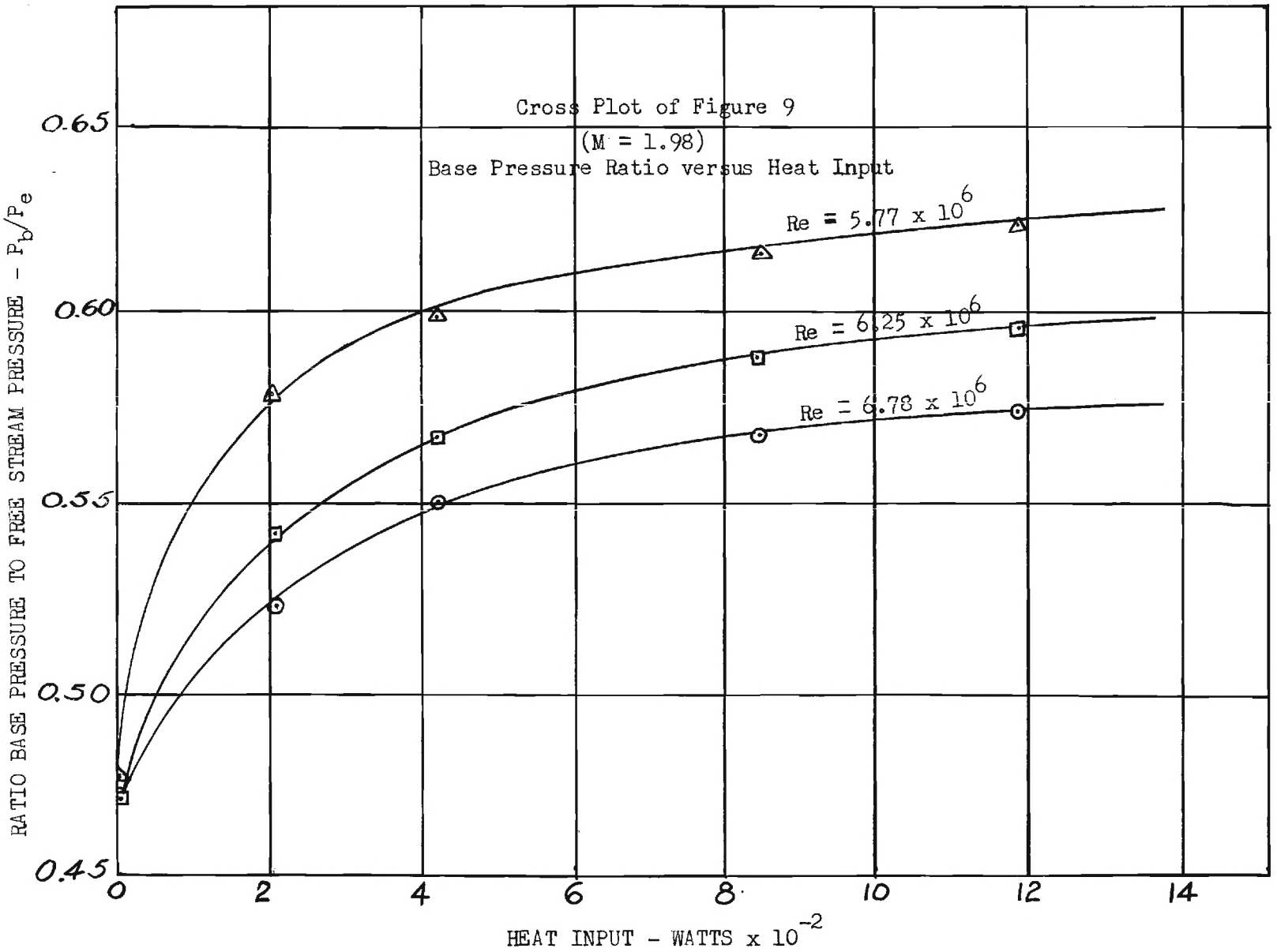
Cross Plot of Figure 9
(M = 1.98)
Base Pressure Ratio versus Heat Input
Re = 5.77 x 10^6
Re = 6.25 x 10^6
Re = 6.78 x 10^6
RATIO BASE PRESSURE TO FREE STREAM PRESSURE - P_b/P_e
0.65
0.60
0.55
0.50
0.45
0
2
4
6
8
10
12
14
HEAT INPUT - WATTS x 10^{-2}

Figure 11

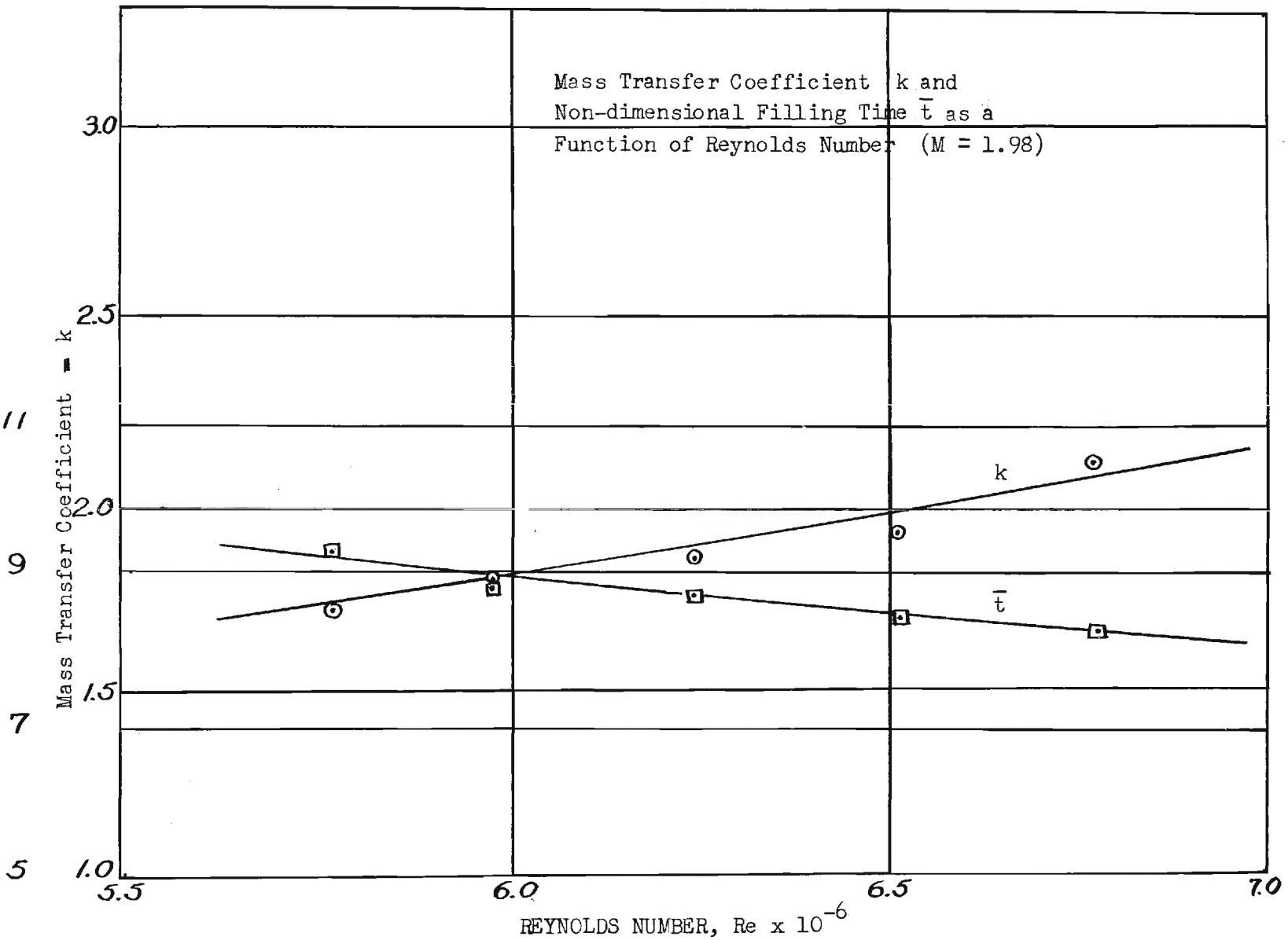
Mass Transfer Coefficient k and
Non-dimensional Filling Time $\bar{t}$ as a
Function of Reynolds Number (M = 1.98)
Mass Transfer Coefficient = k
Non-dimensional Filling Time = $\bar{t}$
3.0
2.5
2.0
1.5
1.0
11
9
7
5
k
$\bar{t}$
5.5
6.0
6.5
7.0
REYNOLDS NUMBER, Re x 10^{-6}

Figure 12

the boundary layer flow is changed to a free jet flow, then it should extract flow from the dead air region; the only portion of the free boundary layer flow which adds mass to the dead air region is that portion of the free flow where the flow is changing from true boundary layer flow to free jet flow. Utilizing the result that this distance is of order 2δ, $C = \mathcal{O}(2\delta)$ and $k_1 \leq k/16$ for $\delta^* = \frac{1}{8}\delta$ (1/7 power law). It can be seen from Figure 13 that $k_1 \approx 0.12$. This checks qualitatively with the value of $k_1 = 0.03$ used by Lees and Crocco for low speed turbulent flow at separation as k_1 (L. and C.) must be $\leq k_1$ from this experiment.

The vented stagnation temperature probe was tested for temperature recovery factor C_θ by recording simultaneously the stagnation temperature T_o far upstream of the tunnel throat and the temperature T_w recorded by the probe mounted in the tunnel test section. The formula used to find the recovery factor was

$$C_\theta = \frac{T_w - T}{T_o - T} \tag{17}$$

where $T = T_o / (1 + \frac{\gamma - 1}{2} M^2)$ from the isentropic formula for static temperature. The values of C_θ varied from 0.96 to 1.0 for various upstream conditions. It is significant that C_θ is very near to unity thus obviating the correction of probe total temperature readings for Mach numbers up to 0.7. The Mach number in the wake was of the order of 0.7 or less. For Mach numbers of the order of 0.7 shock waves begin to appear at the shoulder of probes or wedges placed in the stream. During some runs a blunt probe was placed in the wake. Constant checks of the schlieren screen and negatives failed to reveal the presence of shocks on the probe. Static pressure data were inadequate for measuring the Mach number in the wake although it indicated that

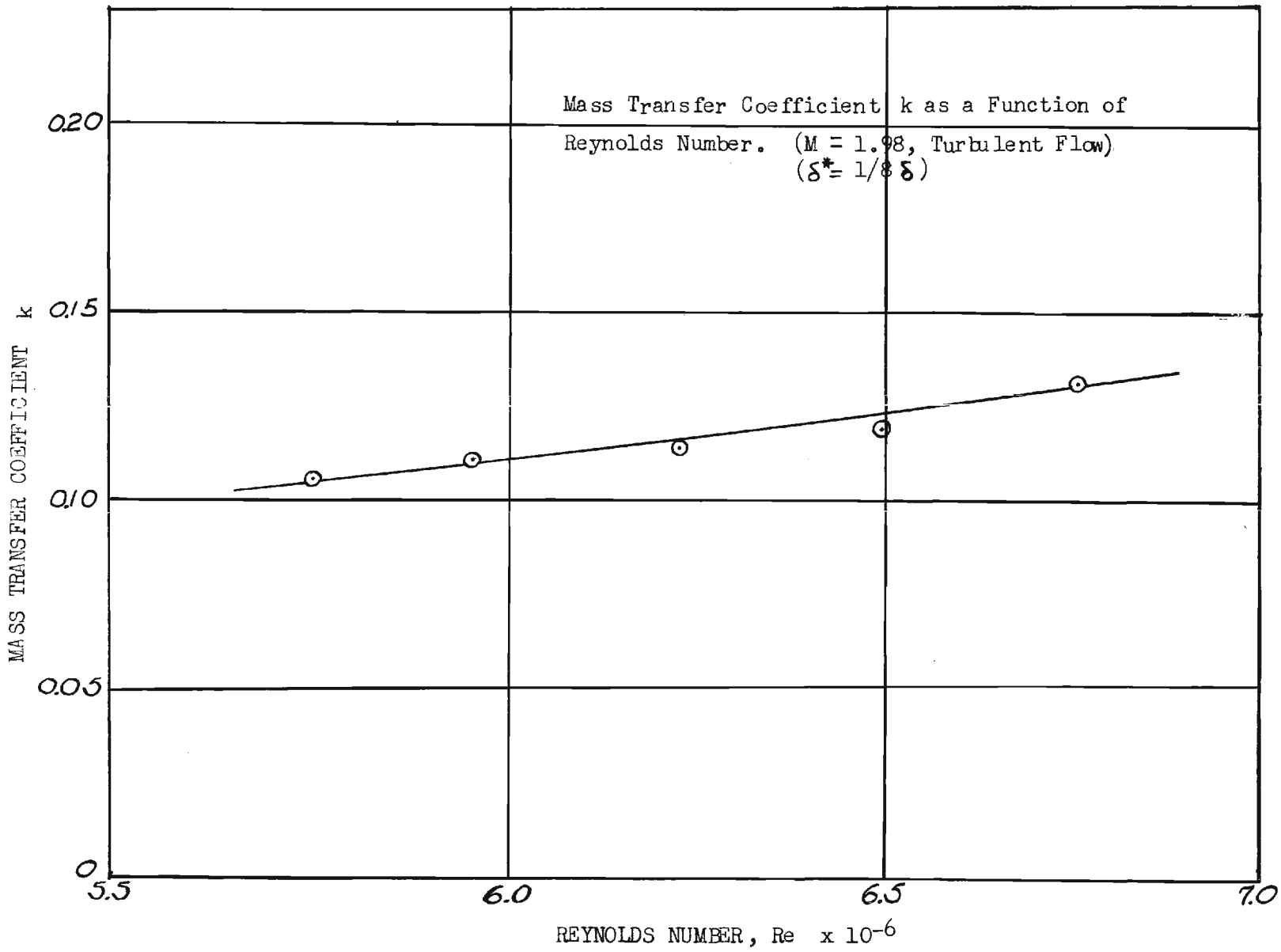
Mass Transfer Coefficient k as a Function of
Reynolds Number. (M = 1.98, Turbulent Flow)
(δ* = 1/8 δ)
MASS TRANSFER COEFFICIENT k
0.20
0.15
0.10
0.05
0
5.5
6.0
6.5
7.0
REYNOLDS NUMBER, Re x 10-6

Figure 13

it was quite low.

The ratios of wake stagnation temperature at various center line positions in the wake to the free stream stagnation temperature are plotted against the flow Reynolds number in Figure 14 for no heat addition. The curves are essentially the same except for a small scatter to the data. They show that the wake stagnation temperatures are less than free stream thus indicating that the mechanism of boundary layer feed into the wake is correct as the average boundary layer stagnation temperature near the wall is less than free stream. There is no change in T_{o_w}/T_o for various positions in the wake upstream of the shock interception point.

The stagnation temperature ratios along the wake center line were also found for a heat addition of 1187 watts at the base. One set of temperatures was taken approximately 4 base widths downstream of the base; this is downstream of the shock interception point. The others were taken adjacent to the base and upstream of the critical section. It was to be expected that the stagnation temperature would drop as the cold boundary layer air was mixed in the wake with the hot air originating at the base of the model. The wake stagnation temperature ratios for various wake positions are plotted in Figure 15. The stagnation temperatures rose slightly as the probe was moved downstream, instead of dropping. This can be explained by the construction of the heating coil; the heating wire was wrapped about two ceramic rods, which were situated in the plane of the center line. The hotter air from the outer portions of the coil is continuously being fed into the secondary dead air region formed by the ceramic rods. However, four base thicknesses downstream the stagnation temperature has dropped perceptibly due to mixing with the outside cold air stream. This slight change in

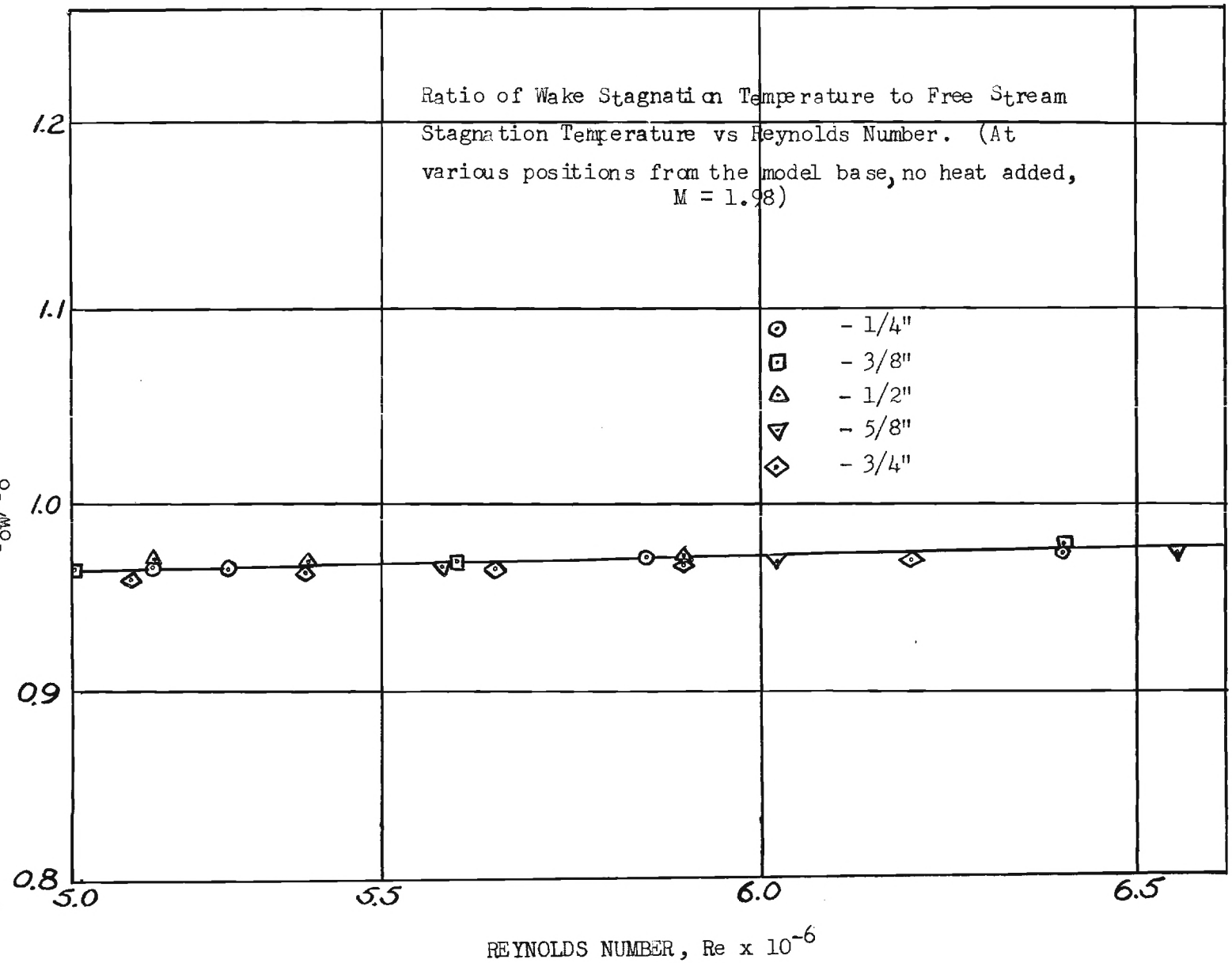
Ratio of Wake Stagnation Temperature to Free Stream Stagnation Temperature vs Reynolds Number. (At various positions from the model base, no heat added, M = 1.98)
- 1/4"
- 3/8"
- 1/2"
- 5/8"
- 3/4"
RATIO WAKE STAGNATION TEMPERATURE TO FREE STREAM STAGNATION TEMPERATURE
T_{ow}/T_o
1.2
1.1
1.0
0.9
0.8
5.0
5.5
6.0
6.5
REYNOLDS NUMBER, Re x 10^{-6}

Figure 14

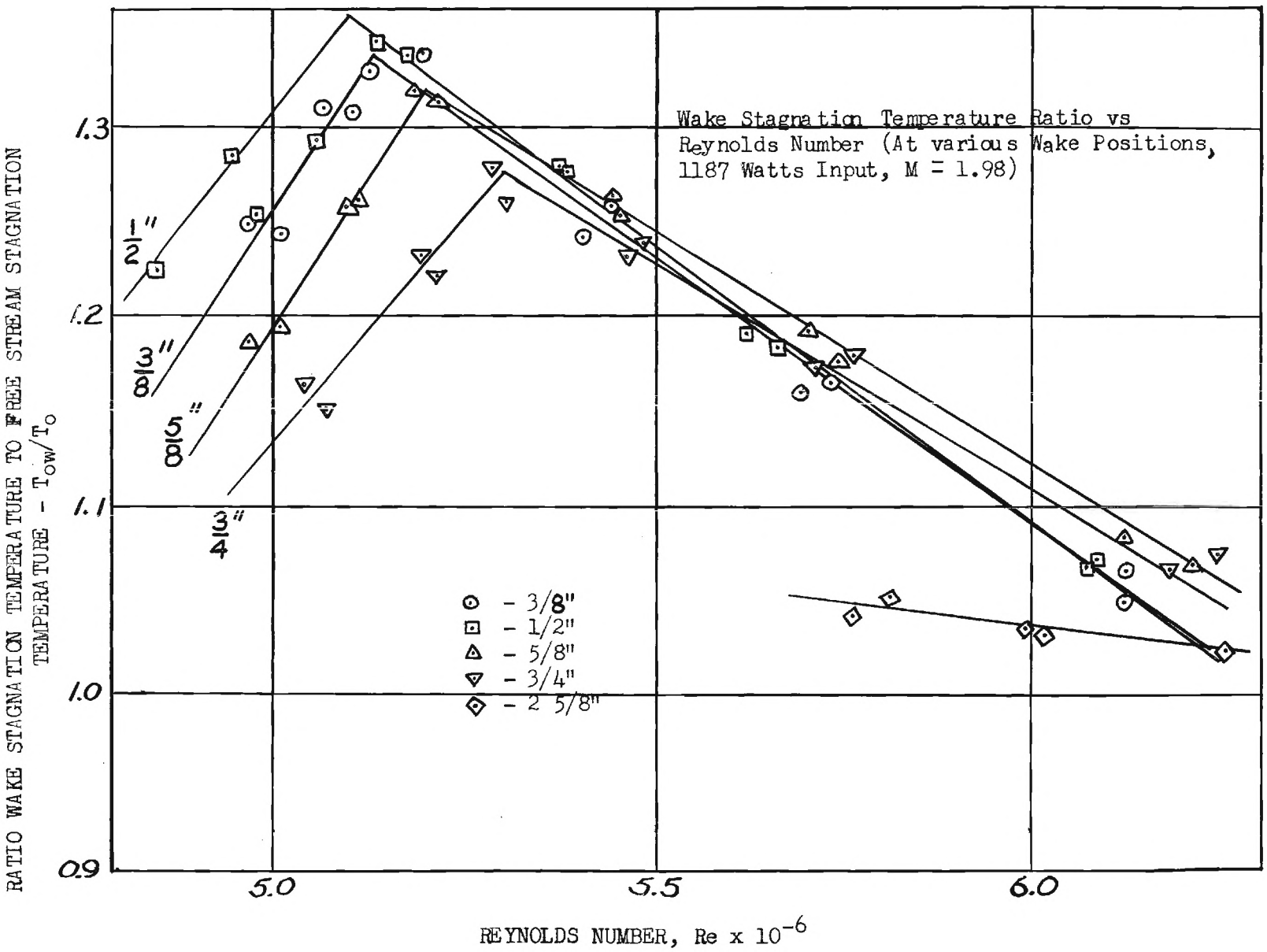
Wake Stagnation Temperature Ratio vs
Reynolds Number (At various Wake Positions,
1187 Watts Input, M = 1.98)
RATIO WAKE STAGNATION TEMPERATURE TO FREE STREAM STAGNATION TEMPERATURE - T_{ow}/T_o
REYNOLDS NUMBER, Re x 10^{-6}
1.3
1.2
1.1
1.0
0.9
5.0
5.5
6.0
1/2"
3/8"
5/8"
3/4"
⊙ - 3/8"
⊡ - 1/2"
△ - 5/8"
▽ - 3/4"
◇ - 2 5/8"

Figure 15

stagnation temperature (total energy) near the base bears out the hypothesis of the decreased mass transfer from the boundary layer due to the analogy between heat and fluid sources.

At the point where the base flow changed from turn-in to turn-out the mass transfer increased rapidly thus bringing more cold air into the wake and reducing the stagnation temperature. As this occurs at a point of instability there is no pattern to the data near this point. This can be seen in Figure 15, where the sudden fall off in stagnation temperature indicates the turn-out point.

Pressure measurements were also made along the wake center line. The flow near the base has high curvature; the flow probably reverses direction within the wake near the center line. Due to vibration of the probes it was difficult to set the probes exactly on the centerline. It would be foolhardy to say that the readings in the wake of the stagnation pressure probe and the static pressure probe gave stagnation and static pressures exactly. Figure 16 shows plots of the pressures measured along the center line by the total pressure probe as a function of distance from the base and Reynolds number for no heat addition. It can be seen that the pressure rises slowly as the flow moves back toward the ultimate wake. Thus there is a small pressure recovery in the base region. The curves at each downstream station exhibit a dip in the vicinity of $Re = 6 \times 10^6$. This dip occurred at the previously mentioned transition point, when violent oscillation of the probe took place.

Figure 17 is a plot of the stagnation pressure versus Reynolds number at the wake centerline 3/4 inch from the base for no base heat addition and 1187 watts heat addition. The pressure was increased, as expected, by heat

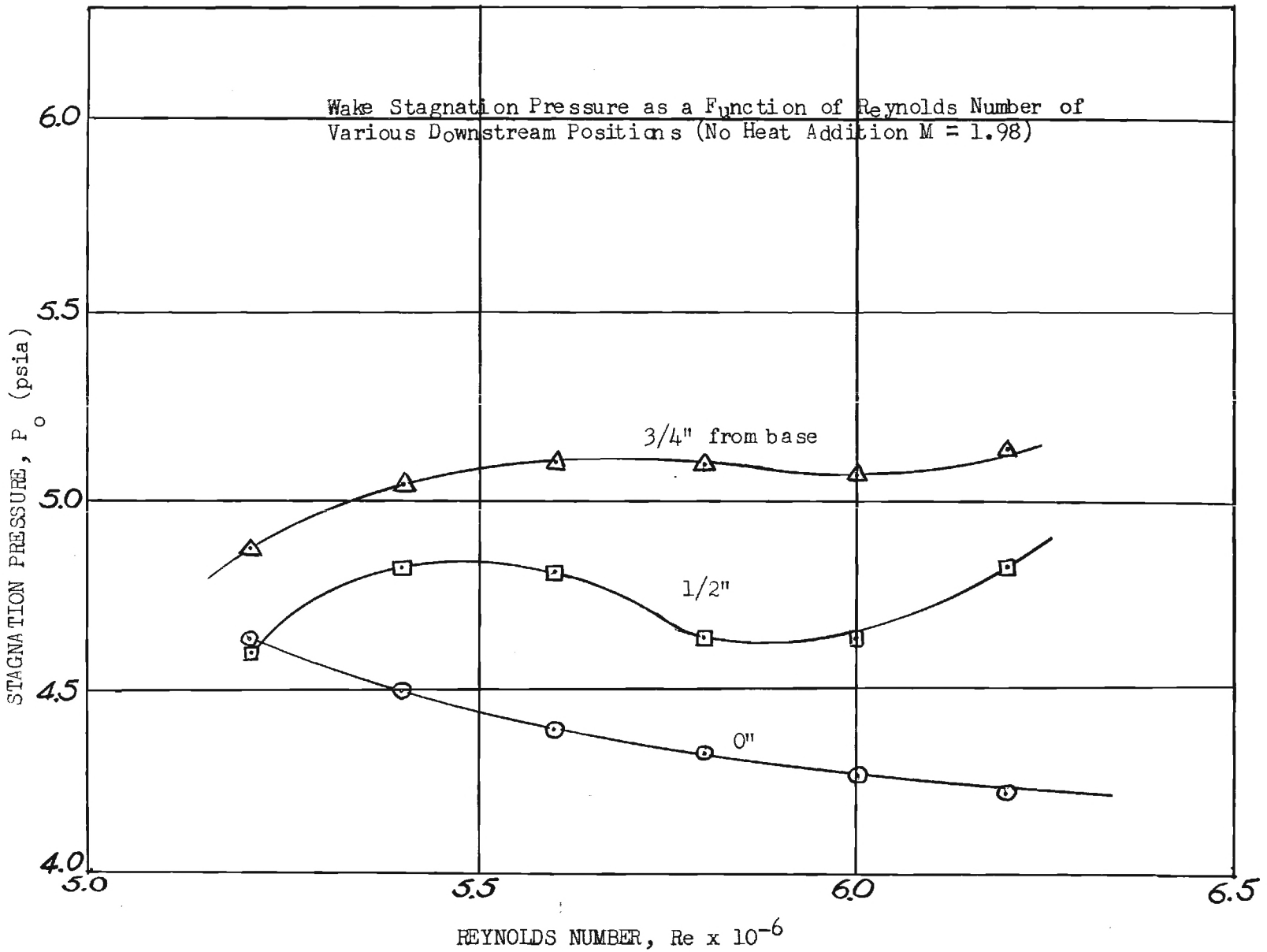
Wake Stagnation Pressure as a Function of Reynolds Number of Various Downstream Positions (No Heat Addition M = 1.98)
STAGNATION PRESSURE, P_o (psia)
6.0
5.5
5.0
4.5
4.0
3/4" from base
1/2"
0"
5.0
5.5
6.0
6.5
REYNOLDS NUMBER, Re x 10^{-6}

Figure 16

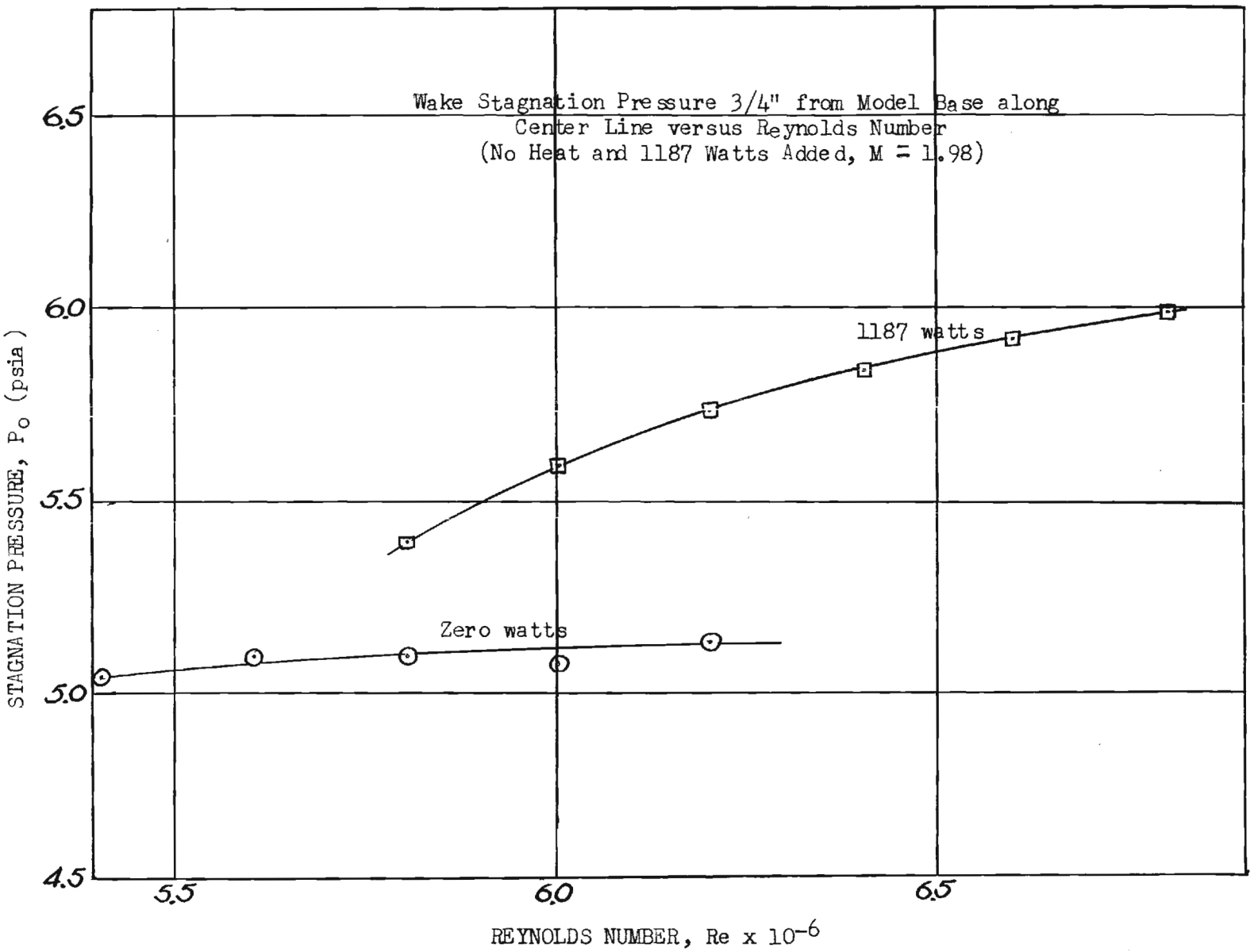
Wake Stagnation Pressure 3/4" from Model Base along
Center Line versus Reynolds Number
(No Heat and 1187 Watts Added, M = 1.98)
1187 watts
Zero watts
6.5
6.0
5.5
5.0
4.5
5.5
6.0
6.5
STAGNATION PRESSURE, P_o (psia)
REYNOLDS NUMBER, Re x 10^{-6}

Figure 17

addition. The oscillation dip disappeared for the heat addition run, which checks with the schlieren observation of the disappearance of probe oscillation at high heat inputs.

The variation of stagnation pressure (nominal stagnation pressure) with downstream distance at Re = 5.8×10^6 for no heat addition and 1187 watts heat addition is shown in Figure 18. The pressure rises with distance away from the base except for a dip near the base. This dip near the base is probably due to the probe not reading true stagnation pressure. This is borne out by the fact that the static pressure probe measured pressures very near in value to those measured by the stagnation pressure probe. The scatter of the static data was so large that no quantitative conclusions could be drawn from it and therefore was not included in this report. However, the magnitude of the static pressure indicated that the Mach number of the flow in the wake was low subsonic.

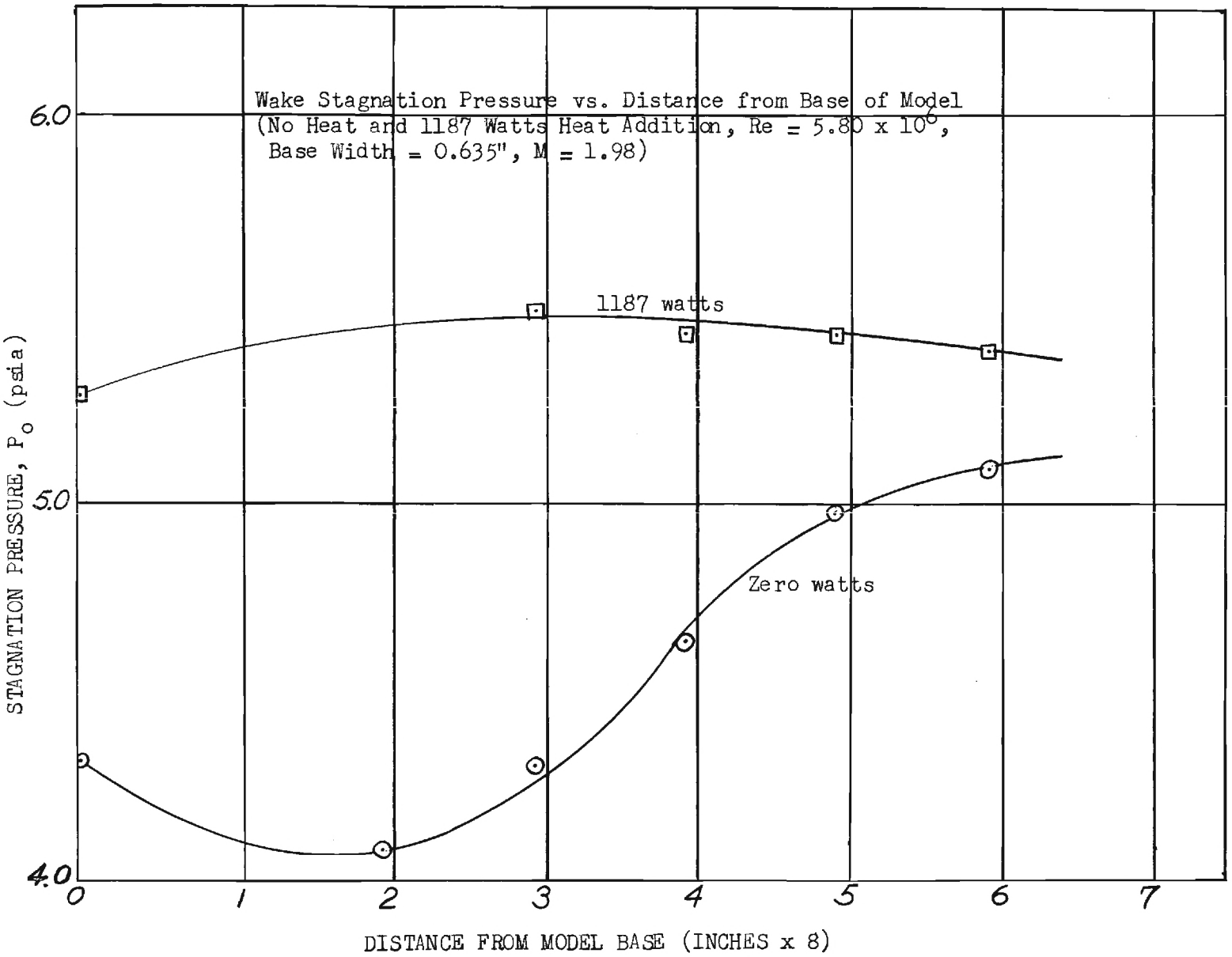
Wake Stagnation Pressure vs. Distance from Base of Model
(No Heat and 1187 Watts Heat Addition, Re = 5.80 x 10^6,
Base Width = 0.635", M = 1.98)
1187 watts
Zero watts
STAGNATION PRESSURE, P_o (psia)
6.0
5.0
4.0
0
1
2
3
4
5
6
7
DISTANCE FROM MODEL BASE (INCHES x 8)

Figure 18

VI. CONCLUSIONS

The base pressure ratio of a blunt-based body in supersonic flow is very sensitive to heat addition at the base. The addition of heat was found to raise the base pressure ratio. The change was not linear with heat addition but tapered off at the higher heat additions; it seems likely that it approaches asymptotically some value of base pressure ratio. If base heat addition were to be used to lower the drag of a blunt-based body, there would be an optimum heat energy input beyond which it would be more economical to add the energy to the flow in some other manner.

The flow at the base was slightly unsteady. This unsteadiness showed up as a slight vibration of probes placed in the wake and by small, long period, waves on the oscillograph pressure records. Addition of small amounts of heat to the base did not change this unsteadiness. However, the flow was steady for medium and large heat additions. We define large amounts of heat as being in the regime where change in heat addition affects the base pressure only slightly. Medium heat is at the edge of the linear portion of the heat-base pressure curve. Thus it should be possible to damp out the wake unsteadiness by heat addition and still be in the favorable section of the curve.

The findings of Chapman, regarding the increase of base pressure of a three-dimensional body, due to intersection of the wake near the base by a shock exterior to the flow proper, were confirmed for a two-dimensional blunt-based body.

The measured values of boundary layer mass transfer are of the same order of magnitude as those employed by Lees and Crocco from subsonic data. This indicates that the simplified theory may be used to predict the effect of heat addition upon the base pressure.

VII. RECOMMENDATIONS

1. The effect of base heat addition upon base pressure should be checked over a wide range of Reynolds numbers in order to find the effect of Reynolds number on the mass transfer coefficient.

2. The axial wake surveys of this report should be augmented by lateral surveys to find the diffusion of heat within the wake.

3. The effect on base pressure of heat addition to the boundary layer should be compared with the results for base addition to find the most efficient method of heat addition.

4. The effect of shock intersections with the wake upon the properties of the wake should be completely explored utilizing shocks, whose strength and position can be varied at will. This should give some insight into the properties and position of the wake critical section.

Respectfully submitted:

Richard G. Fledderman
Project Director

Approved:

for Paul K. Calaway, Acting Director
Engineering Experiment Station

Hurlbut W. S. LaVier
Research Associate

VIII. BIBLIOGRAPHY

1. Carrier, G. F., and Lin, C. C., "On the Nature of the Boundary Layer near the Leading Edge of a Flat Plate." Quarterly of Applied Mathematics, 6, pp. 63-68, (1948).

2. Chapman, Dean R., An Analysis of Base Pressure at Supersonic Velocities and Comparison with Experiment, N. A. C. A. Technical Note 2137, July, 1950.

3. Chapman, D. R., Winbrow, W. R. and Kester, R. H., Experimental Investigation of Base Pressure on Blunt-Trailing-Edge Wings at Supersonic Velocities, N. A. C. A. Technical Note 2611, January, 1952.

4. Crocco, Luigi and Lees, Lester, "A Mixing Theory for the Interaction between Dissipative Flows and Nearly Isentropic Streams." Journal of the Aeronautical Sciences, 19, 649-677, (1952).

5. Goldstein, Sidney, "On Laminar Boundary Layer Flow Near a Position of Separation." Quarterly Journal of Mechanics, 1, 43-69, (1948).

6. Hicks, B. L., Hebrank, W. H. and Kravitz, S., "On the Characterization of Fields of Diabatic Flow," Part II, Ballistics Research Laboratories Report No. 720, July, 1950.

7. Holder, D. W., North, R. J. and Chinneck, A., Experiments with Static Tubes in a Supersonic Air Stream, Parts I and II, Reports and Memoranda No. 2782, British Research Council, (1953).

8. Stewartson, K., "On the Flow Downstream of Separation in an Incompressible Fluid." Proceedings of the Cambridge Philosophical Society, 49, 561-569, (1953).

9. Stewartson, K., "Correlated Incompressible and Compressible Boundary Layers." Proceedings of the Royal Society of London, A-200, 84-100, (1949).

DISTRIBUTION LIST

No. of Copies	Addressee
10	Office of Ordnance Research Box CM, Duke Station Durham, North Carolina
1	Office, Chief of Ordnance Washington 25, D. C. Attn: ORDTB-PS
1	Commanding General White Sands Proving Ground Las Cruces, New Mexico
1	Office of Naval Research Washington 25, D. C.
2	Commanding General Aberdeen Proving Ground, Maryland Attn: BRL
1	Commanding General Redstone Arsenal Huntsville, Alabama
1	Chief, Ordnance Development Div. National Bureau of Standards Washington 25, D. C.
1	Commanding Officer Watertown Arsenal Watertown 72, Mass.
1	Commanding Officer Engineer Res. & Dev. Laboratories Fort Belvoir, Virginia
1	Canadian Joint Staff 1700 Massachusetts Ave., N. W. Washington 6, D. C. Thru: ORDGU-SE
1	Commanding General Air Res. & Dev. Command P. O. Box 1395 Baltimore 3, Maryland Attn: RDD

Distribution List (Continued)

No. of Copies	Addressee
1	Commanding General Air Res. & Dev. Command P. O. Box 1395 Baltimore 3, Maryland Attn: RDR
5	Armed Services Tech. Info. Agency Document Service Center Knott Building Dayton 2, Ohio Attn: DSC-SD
1	Commander U. S. Naval Ord Test Station, Inyokern China Lake, California Attn: Technical Library
1	U. S. Atomic Energy Commission Document Library 19th & Constitution Ave. Washington 25, D. C.
1	Commanding General Air Material Command Wright-Patterson Air Force Base Dayton 2, Ohio Attn: F. N. Bubb, Chief Scientist Flight Research Lab
1	NAC for Aeronautics 1724 F Street, N. W. Washington 25, D. C. Attn: Mr. E. B. Jackson, Chief Office of Aero. Intelligence
1	Scientific Information Section Research Branch Research & Development Division Office, Assistant Chief of Staff, G-4 Department of the Army Washington 25, D. C.